THE JOURNAL OF BIOLOGICAL CHEMISTRY VOL. 289, NO. 52, pp. 36204–36219, December 26, 2014
Published in the U.S.A.

Modulation of the Mevalonate Pathway by Akt Regulates Macrophage Survival and Development of Pulmonary Fibrosis*

Received for publication, June 30, 2014, and in revised form, October 24, 2014 Published, JBC Papers in Press, November 5, 2014, DOI 10.1074/jbc.M114.593285

Jennifer L. Larson-Casey[‡], Shubha Murthy[§], Alan J. Ryan[§], and A. Brent Carter[‡§¶‖1]

From the [‡]Department of Radiation Oncology and Program in Free Radical and Radiation Biology, the [§]Department of Internal Medicine, Carver College of Medicine, and the [¶]Department of Human Toxicology, College of Public Health, University of Iowa, Iowa City, Iowa 52242 and the [‖]Iowa City Veterans Affairs Health Care System, Iowa City, Iowa 52242

Background: The serine/threonine protein kinase Akt and the mevalonate pathway are both linked to cell survival.
Results: Akt activates the mevalonate pathway, and this relationship enhanced macrophage survival.
Conclusion: Macrophage survival was found in patients with pulmonary fibrosis and in mice with a fibrotic phenotype.
Significance: These observations provide a novel target for preventing the development of pulmonary fibrosis by regulating Akt activation in alveolar macrophages.

Protein kinase B (Akt) is a key effector of multiple cellular processes, including cell survival. Akt, a serine/threonine kinase, is known to increase cell survival by regulation of the intrinsic pathway for apoptosis. In this study, we found that Akt modulated the mevalonate pathway, which is also linked to cell survival, by increasing Rho GTPase activation. Akt modulated the pathway by phosphorylating mevalonate diphosphate decarboxylase (MDD) at Ser^{96}. This phosphorylation in macrophages increased activation of Rac1, which enhanced macrophage survival because mutation of MDD (MDD_{S96A}) induced apoptosis. Akt-mediated activation in macrophages was specific for Rac1 because Akt did not increase activity of other Rho GTP-binding proteins. The relationship between Akt and Rac1 was biologically relevant because $Akt^{+/-}$ mice had significantly less active Rac1 in alveolar macrophages, and macrophages from $Akt^{+/-}$ mice had an increase in active caspase-9 and -3. More importantly, $Akt^{+/-}$ mice were significantly protected from the development of pulmonary fibrosis, suggesting that macrophage survival is associated with the fibrotic phenotype. These observations for the first time suggest that Akt plays a critical role in the development and progression of pulmonary fibrosis by enhancing macrophage survival via modulation of the mevalonate pathway.

The serine/threonine protein kinase Akt, also known as protein kinase B (PKB), is part of a well established pro-survival pathway mediating cell growth, metabolism, and reactive oxygen species (ROS)[2] production (1). Akt is known to phosphorylate many proteins and thereby alter the regulation of apoptosis. Inactivation of the proapoptotic factors, BAD (2, 3) and caspase-9 (4), by Akt phosphorylation has been well studied. Similarly, Akt phosphorylates the FOXO transcription factor, leading to its inactivation and inability to regulate the expression of proapoptotic genes, such as the FAS receptor (5), Mdm2 (6), and p53 (7). The close association of Akt with cellular death and survival is associated with its augmented expression in many human diseases.

The hyperactivation of Akt is associated with many human cancers, diabetes, and neurodegenerative disorders (8, 9). Akt has also been shown to be up-regulated in various fibrotic tissues (10–12). Specifically, Akt is increased in bleomycin-stimulated fibroblasts *in vitro* (11) and *in vivo* (13–15) and in idiopathic pulmonary fibrosis fibroblasts (13), and Akt deficient mice display less lung injury in a high tidal volume model (12). However, there is no direct link between Akt activation in alveolar macrophages and the development of pulmonary fibrosis.

The mevalonate pathway is widely known for its role in sterol biosynthesis; millions are prescribed statins annually to treat hypercholesterolemia. Besides cardiovascular disease, the mevalonate pathway has also been implicated in many other human diseases, and several pharmaceutical agents have been designed to target enzymes in this pathway (16–19). In particular, compounds have been developed for cancer therapy because the mevalonate pathway also increases cell survival (20, 21).

In this study, we examined the relationship between Akt and several Rho GTP proteins. GTP-binding proteins are post-translationally modified by the addition of either a farnesyl or geranylgeranyl derivative to the C-terminal cysteine residue. This lipidation process is necessary for activation and localiza-

* This work was supported, in whole or in part, by National Institutes of Health Grants 2R01ES015981-07 (to A. B. C.), T32CA078586 (to the Free Radical and Radiation Biology Program), and P30CA086862 (to the University of Iowa Comprehensive Cancer Center). This work was also supported by Department of Veterans Affairs, Veterans Health Administration, Office of Research and Development, Biological Laboratory Research and Development Merit Review Grant 1BX001135-01 (to A. B. C.).

[1] To whom correspondence should be addressed: University of Iowa Carver College of Medicine, Iowa City Veterans Affairs Health Care System, 200 Hawkins Dr., Iowa City, IA 52242. Tel.: 319-384-4557; Fax: 319-353-6406; E-mail: brent-carter@uiowa.edu.

[2] The abbreviations used are: ROS, reactive oxygen species; MDD, mevalonate diphosphate decarboxylase; DGBP, digeranyl bisphosphonate; BAL, bronchoalveolar lavage; GGDP, geranylgeranyl diphosphate; PEG-CAT, polyethylene glycol-conjugated catalase; GTPγS, guanosine 5′-3-*O*-(thio)triphosphate.

tion of Rho GTPase proteins (22–24), and inhibition of protein geranylgeranylation induces cell death (25–27). The persistent activation of GTPases has been shown to promote tumorigenesis through uncontrolled cell proliferation, migration, and invasion while simultaneously inhibiting apoptosis (20).

The relationship between Akt and Rho GTP-binding proteins is not clear because they have been shown to both positively and negatively modulate each other (28–33). In the present study, we show that in alveolar macrophages, Akt directly regulates the mevalonate pathway by phosphorylating mevalonate diphosphate decarboxylase (MDD), a critical protein in the pathway. Akt specifically modulates Rac1 geranylgeranylation and activity and protects alveolar macrophages from apoptosis in a Rac1-dependent manner. Furthermore, mice deficient in Akt have reduced Rac1 activity and increased apoptosis and are protected from fibrosis development. These novel observations provide a new mechanistic target for preventing the occurrence of pulmonary fibrosis by regulating Akt activation in alveolar macrophages.

EXPERIMENTAL PROCEDURES

Materials—Chrysotile asbestos was provided by Dr. Peter S. Thorne University of Iowa). Digeranyl bisphosphonate (DGBP; United States patent 7,268,164) was generously provided by Jeffrey D. Neighbors and Raymond Hohl (University of Iowa). *p*-Hydroxylphenyl acetic acid, horseradish peroxidase (HRP), α-ketoglutarate, cholesterol, LY-294,200 hydrochloride, NADPH, polyethylene glycol-conjugated catalase (PEG-CAT), Triton X-100, and Triton X-114 were purchased from Sigma.

Human Subjects—The Human Subjects Review Board of the University of Iowa Carver College of Medicine approved the protocol of obtaining alveolar macrophages from normal volunteers and patients with asbestosis. Normal volunteers had to meet the following criteria: 1) age between 18 and 55 years; 2) no history of cardiopulmonary disease or other chronic disease; 3) no prescription or nonprescription medication except oral contraceptives; 4) no recent or current evidence of infection; and 5) lifetime nonsmoker. Patients had to meet the following criteria: 1) FVC (forced vital capacity) and DLCO (diffusion capacity of the lung for CO) at least 50% predicted; 2) current nonsmoker; 3) no recent or current evidence of infection; and 4) evidence of restrictive physiology on pulmonary function tests and interstitial fibrosis on chest computed tomography. Fiberoptic bronchoscopy with bronchoalveolar lavage was performed after subjects received intramuscular atropine (0.6 mg) and local anesthesia. Each subsegment of the lung was lavaged with five 20-ml aliquots of normal saline, and the first aliquot in each was discarded. The percentage of alveolar macrophages was determined by Wright-Giemsa stain and varied from 90 to 98%.

Mice—Wild-type C57BL/6 and Akt1$^{+/-}$ mice (B6.129P2-Akt1tm1Mbb/J) were purchased from Jackson Laboratories. All protocols were approved by the University of Iowa Institutional Animal Care and Use Committee. Mice were intratracheally administered 100–125 μg of chrysotile asbestos suspension in 50 μl of 0.9% saline solution after being anesthetized with 3% isoflurane using a precision Fortec vaporizer (Cyprane, Keighley, UK). Mice were euthanized 21 days after exposure to chrysotile with an overdose of isoflurane. Bronchoalveolar lavage (BAL) was performed, and BAL cells were used for determination of total and cell differential numbers, whereas BAL fluid was used for determination of cytokine concentrations. The lungs were removed and stained for collagen fibers using Masson's trichrome.

Cell Culture—Human monocyte (THP-1), mouse alveolar macrophage (MH-S), and human lung fibroblast (HLF-1) cell lines were obtained from the American Type Culture Collection. Cells were maintained in RPMI 1640 medium with 2–10% fetal bovine serum and penicillin/streptomycin supplements. All experiments were conducted in RPMI containing 0.5% serum.

Plasmids and Transfections—The constitutively active Akt (NM_005163.2) plasmid (Akt) was a generous gift from Rama K. Mallampalli (Department of Medicine, University of Pittsburgh). The full-length human Rac1 (NM_006908.3) was amplified with PCR using Rac1 cDNA in pUSEamp (Millipore) as a template plus forward and reverse primers containing 5′-NheI or 3′-EcoRV sites. The resulting PCR product was cloned into pCR4-TOPO (Invitrogen), digested, and then ligated into the NheI-EcoRV sites of the phMGFP vector. The phMGFP construct contains a GFP epitope on the N terminus. pRK-FLAG-Rac1 was described previously (24). Constitutively active Rac1 plasmid was purchased from Millipore. Full-length human MDD (NM_002461.1) plasmid was purchased from Origene. Mutations of serine residues were generated using the QuikChange® Lightning multisite-directed mutagenesis kit (Agilent Technologies). Using PCR techniques, full-length MDD and the generated constructs were directionally cloned into pcDNA3.1D/V5-His-TOPO vector (Invitrogen). The following constructs were generated: MDD_{WT}, MDD_{S96A}, MDD_{S231A}, and $MDD_{S96A,S231A}$. The correct reading frame and sequence of all plasmids used in the study were verified by fluorescent automated DNA sequencing performed by the University of Iowa DNA Facility. Cells were transfected using X-treme GENE 9 Transfection Reagent (Roche Applied Science) according to the manufacturer's protocol.

Determination of H_2O_2 Generation—H_2O_2 production was determined fluorometrically, as described previously (34). Mitochondrial H_2O_2 was measured by resuspending mitochondria in phenol-red free Hanks' balanced salt solution supplemented with 6.5 mM glucose, 6 mM HEPES, 6 mM sodium bicarbonate, 1.6 mM *p*-hydroxylphenyl acetic acid, 0.95 μg/ml HRP, and 5 mM α-ketoglutarate. Fluorescence of the *p*-hydroxylphenyl acetic acid dimer was measured using a spectrofluorometer at excitation of 320 nm and emission of 400 nm.

Isolation of Mitochondria and Cytoplasm—Cell fractions were prepared as described previously (35, 36).

Synthesis of DGBP—DGBP (U.S. Patent 7,268,164) was synthesized as described previously (37).

Triton X-114 Separation—The separation of geranylgeranylated and non-geranylgeranylated Rac1 was prepared according to a previously published protocol (38). Briefly, cells were lysed in ice-cold Triton X-114 lysis buffer (20 mM Tris, pH 7.5, 150 mM NaCl, and 1% Triton X-114). Cell lysates were sonicated and cleared by centrifugation. The supernatant was incubated at 37 °C for 10 min and centrifuged at room temperature for 2

min at 12,000 × *g*. The detergent or lower phase was diluted with buffer that did not contain Triton X-114, and the aqueous or upper phase was transferred to a new tube.

Immunoblot Analysis—Cell protein lysates were harvested in lysis buffer containing a protease inhibitor mix (Roche Applied Science, Complete Mini tablets) and a phosphatase inhibitor mix (Calbiochem), unless otherwise stated. Cell lysates were assayed for protein content using a DC™ protein assay kit (Bio-Rad). Whole cell lysates, subcellular fractions, and conditioned medium were separated by SDS-PAGE and transferred to PVDF membranes. Immunoblot analyses on the membranes were performed with the designated antibodies, followed by the appropriate secondary antibody cross-linked to horseradish peroxidase. Primary antibodies used were as follows: rabbit polyclonal anti-phospho-Akt (Ser^{473}), rabbit polyclonal anti-Akt, rabbit monoclonal anti-caspase-3 (8G10), mouse monoclonal anti-caspase-9 (C9), and rabbit polyclonal anti-voltage-dependent anion channel (Cell Signaling); rabbit polyclonal anti-collagen α2 type I (H-70) and goat polyclonal anti-Rap 1A (C17) (Santa Cruz Biotechnology, Inc.); mouse polyclonal anti-collagen type I, mouse monoclonal anti-GAPDH (6C5), mouse monoclonal anti-phosphoserine (4A4), and mouse monoclonal anti-Rac1 (23A8) (Millipore); rabbit polyclonal anti-MDD (Abnova or Origene); mouse monoclonal anti-$gp91^{phox}$ (BD Biosciences); mouse monoclonal anti-UQCRFS1 (5A5) (anti-Rieske) (Abcam); mouse monoclonal anti-V5 (Invitrogen); and mouse monoclonal anti-β-actin (AC-15) (Sigma).

Purification of MDD-V5-His-tagged Protein—Cells were transfected with empty pcDNA3.1, constitutively active Akt, or pcDNA3.1-MDD-V5-His vectors. Cells were harvested in Buffer B (10 mM Tris-HCl, pH 7.5, 0.5 M NaCl, 5 mM imidazole, and 1% Triton X-100 plus protease and phosphatase inhibitors). Lysates were briefly sonicated on ice, and cellular debris was pelleted at 12,000 × *g* for 10 min at 4 °C. Talon metal (cobalt) affinity resin (Clontech) was added to each lysate, and samples were rotated at 4 °C for 2 h and then washed three times with Buffer B. MDD-V5-His proteins were eluted by adding protein sample buffer and heating at 95 °C for 5 min.

Qualitative Real-time PCR—Total RNA was isolated using TRIzol reagent (Sigma) and reverse transcribed using iScript reverse transcription kit (Bio-Rad). mRNA expression was determined by qualitative real-time PCR using the SYBR Green kit (Bio-Rad). The following primer sets were used: human TGF-β1, 5′-CGT GGA GCT GTA CCA GAA ATA C-3′ and 5′-CAC AAC TCC GGT GAC ATC AA-3′; human hypoxanthine-guanine phosphoribosyltransferase, 5′-CCT CAT GGA CTG ATT ATG GAC-3′ and 5′-CAG ATT CAA CTT GCG CTC ATC-3′; mouse TNF-α, 5′-CAC TTG GTG GTT TGC TAC GA-3′ and 5′-CCA CAT CTC CCT CCA GAA AA-3′; mouse Ym1, 5′-TGT TCT GGT GAA GGA AAT GCG-3′ and 5′-CGT CAA TGA TTC CTG CTC CTG-3′; mouse arginase I, 5′-CAG AAG AAT GGA AGA GTC AG-3′ and 5′-CAG ATA TGC AGG GAG TCA CC-3′; mouse β-actin, 5′-AGA GGG AAA TCG TGC GTG AC-3′ and 5′-CAA TAG TGA TGA TGA CCT GGC CGT-3′; mouse IL-1β, 5′-GAT CCA CAC TCT CCA GCT GCA-3′ and 5′- CAA CCA ACA AGT GAT ATT CTC CAT G-3′ Data were calculated by the cycle threshold ($\Delta\Delta C_t$) method. The mRNA measurements were normalized to β-actin or hypoxanthine-guanine phosphoribosyltransferase and expressed in arbitrary units.

ELISA—MCP-1, TGF-β1, TNF-α, and Ym1 in BAL fluid from WT and $Akt^{+/-}$ mice were measured using ELISA kits (R&D Systems) according to the manufacturer's instructions.

Small Interfering RNA (siRNA)—THP-1 cells were transfected with 100 nM scramble, human Akt1, human Rieske siRNA duplex (IDT), or SMARTpool: siGenome human Rac1 siRNA (Thermo Scientific) utilizing Dharmafect 2 or Duo (Thermo Scientific) according to the manufacturer's protocol. 8 h after transfection, medium was replaced, and cells were allowed to recover for 24–72 h.

Rho GTPase Activation Assays—Rac1 activity was determined using the G-LISA kit (Cytoskeleton Inc.), or Rac1, Rac2, and RhoA activity were determined using a bead pull-down kit (Cytoskeleton Inc.), according to the manufacturer's protocols. Negative and positive lysate controls were incubated with GTPγS or GDP, respectively, during PAK-binding domain-GST pull-down for Rac1 and -2 or with Rho-binding domain-GST for RhoA pull-down. Bound protein was eluted and analyzed by SDS-PAGE; GST expression was determined by Coomassie staining as a loading control. Active Rac1 was determined in membrane, cytoplasm, and mitochondria fractions by the binding of Rac1 to PAK-PBD beads immobilized in a 96-well plate using the G-LISA kit.

Caspase-3 Activity Assay—Caspase-3 activity was measured using EnzChek Caspase-3 Assay Kit Number 2 (Molecular Probes) according to the manufacturer's protocol. Briefly, cells were lysed in 1× lysis buffer, subjected to a freeze-thaw cycle, centrifuged to remove cellular debris, and loaded into individual microplate wells. The 2× reaction buffer with substrate was immediately added to the samples, and fluorescence was measured (excitation/emission 496/520 nm). A supplied inhibitor was used as a negative control in all experiments.

TUNEL Assay—Cells were cotransfected with pcDNA3.1 empty or the constitutively active Akt plasmid together with the phMGFP-empty plasmid on a coverglass chamber. Cells were treated with 10 μM DGBP or DMSO overnight. The TUNEL assay was performed using the *in situ* cell death detection system, TMR Red (Roche Applied Science) according to the manufacturer's instructions. Briefly, cells were washed with PBS and then fixed in 3.7% paraformaldehyde in PBS, pH 7.4, for 60 min at room temperature. Fixed cells were washed with PBS and permeabilized using 0.1% Triton X-100 in 0.1% sodium citrate for 2 min at 4 °C. Cells were then treated with the TUNEL reaction mixture for 60 min at 37 °C in a humidified chamber. Cells were washed with PBS and blocked using 5% normal goat serum in PBS for 60 min at room temperature. Following washing, cells were stained using rabbit anti-GFP antibody-Alexa Fluor (Invitrogen) for 60 min at room temperature. Cells were washed with PBS and captured by confocal microscopy using a Zeiss LSM 510 confocal microscope with the 488- and 579-nm lines of a krypton/argon laser used for measuring the fluorescence excitation of GFP and TUNEL, respectively. Controls consisted of cells alone, GFP only-expressing cells, and cells treated only with TUNEL reaction mixture. For positive controls, cells were treated with DNase I (New England BioLabs) at 4 units/ml for 10 min at room temperature

to induce DNA strand breaks. ImageJ software was used to analyze images.

Glutathione Assay—Reduced (GSH) and oxidized glutathione (GSSG) in the lung were determined as described previously (35).

Hydroxyproline Determination—Lung tissue was dried to a stable weight and acid-hydrolyzed with 6 N HCl for 24 h at 112 °C. Hydroxyproline concentration was normalized to the dry weight of the lung, as described previously (39).

Statistical Analysis—Statistical comparisons were performed using either an unpaired two-tailed *t* test or one-way analysis of variance with Tukey's *post hoc* test. All statistical analysis was expressed ± S.D., and $p < 0.05$ was considered to be significant.

RESULTS

$Akt^{+/-}$ Mice Are Protected from Pulmonary Fibrosis—Akt is known to be activated in bleomycin-stimulated fibroblasts *in vitro* (11) and *in vivo* (13–15) and in idiopathic pulmonary fibrosis fibroblasts (13). Akt-deficient mice display less lung injury in a high tidal volume model (12); however, there is no direct link between Akt activation in alveolar macrophages and the development of pulmonary fibrosis. We determined the biological effect of macrophage Akt activation in the pathogenesis of pulmonary fibrosis. WT and $Akt^{+/-}$ mice were exposed to chrysotile asbestos to evaluate fibrotic development. The lungs from WT mice had dense collagen deposition and destruction of normal lung architecture (Fig. 1*A*). Although small areas of collagen accumulation were present, the collagen deposition was drastically reduced, and the lung architecture was preserved in the $Akt^{+/-}$ mice (Fig. 1*B*). The histopathological observations were verified biochemically. Hydroxyproline content in the lungs of WT mice was significantly higher compared with $Akt^{+/-}$ mice, indicating that Akt deficiency limits collagen deposition and pulmonary fibrosis (Fig. 1*C*).

BAL was performed 21 days after chrysotile exposure. $Akt^{+/-}$ mice had a significant decrease in the total number of BAL cells compared with WT mice (Fig. 1*D*); however, alveolar macrophages were the predominant (>90%) cell type in BAL fluid in both WT and $Akt^{+/-}$ mice (Fig. 1*E*). Because $Akt^{+/-}$ mice had a decreased total number of BAL cells, we determined whether these mice had altered macrophage migration or infiltration to the lung. Using BAL fluid, we measured monocyte chemoattractant protein-1 (MCP-1), a key chemokine required for immunological surveillance of tissues and secreted in response to inflammatory stimuli. MCP-1 activity was similar in BAL fluid from WT and $Akt^{+/-}$ mice, suggesting that macrophage recruitment is not altering the reduction of the total number of BAL cells in Akt-deficient mice (Fig. 1*F*).

To verify that $Akt^{+/-}$ mice have decreased Akt activity, macrophages from WT and $Akt^{+/-}$ mice were isolated, and immunoblot analysis revealed that Akt activation as well as total Akt expression were reduced in $Akt^{+/-}$ mice (Fig. 1*G*).

Because the release of H_2O_2 by alveolar macrophages plays an integral role in the pathogenesis of pulmonary fibrosis and the mitochondria are the primary site for its generation (35, 40), we questioned whether ROS levels were associated with Akt deficiency *in vivo*. Mitochondria isolated from alveolar macrophages obtained from $Akt^{+/-}$ mice had significantly reduced mitochondrial H_2O_2 generation compared with the mitochondria obtained from WT mice (Fig. 1*H*).

Because WT and $Akt^{+/-}$ mice had significant differences in mitochondrial H_2O_2 generation, we determined whether alveolar macrophage mitochondrial ROS modulated whole lung oxidative stress. WT and $Akt^{+/-}$ mice were exposed to chrysotile, and lungs were excised and homogenized to determine reduced GSH as well as the percentage of total GSH in the disulfide form (percentage of GSSG). Akt-deficient mice had an increase in reduced GSH levels compared with WT mice, suggesting an increase in glutathione production (Fig. 1*I*). In contrast, the lungs from WT mice had a significantly greater percentage of total glutathione in the oxidized disulfide form (percentage of GSSG) than the lungs from $Akt^{+/-}$ mice (Fig. 1*J*). In aggregate, these data strongly suggest that $Akt^{+/-}$ mice have reduced lung oxidative stress and are protected from developing pulmonary fibrosis.

Akt Specifically Regulates Rac1 Activity—Because Akt-deficient mice are protected from developing pulmonary fibrosis, we investigated the mechanism modulating this protection. Macrophages were exposed to chrysotile asbestos, and Akt activation was analyzed. Activation of Akt was significantly increased in macrophages exposed to chrysotile, and overexpression of constitutively active Akt expression vector further increased Akt activation (Fig. 2*A*). Using the PI3K inhibitor, LY-294002, Akt activation was inhibited below control levels.

Because the Akt pathway is involved in many cellular processes, including cell survival and oxidative stress, and Rho GTP-binding proteins have been linked to fibrosis development, we determined whether Akt regulated the activity of the most prominent Rho GTPase proteins (Rac2, RhoA, and Rac1) in macrophages (24, 34, 39, 41–43). Studies show that Akt and Rho GTP-binding proteins both positively and negatively regulate each other (28, 31–33). Using a pull-down assay in which only the active GTPase binds to the beads, we found that overexpression of Akt decreased Rac2 activity (Fig. 2*B*) and had no significant effect on RhoA activity (Fig. 2*C*). In contrast, Rac1 activity was greatly induced in cells overexpressing Akt (Fig. 2*D*). Activation of Akt was verified by immunoblot analysis of phospho-Akt (Fig. 2, *B–D*, *insets*). To quantify these differences, GTPase activity was expressed as the ratio of active GTPase to GST by densitometry of the immunoblot analyses from three separate experiments (Fig. 2, *B–D*). Because overexpression of Akt up-regulated Rac1 activity, we determined whether inactivation of Akt by siRNA knockdown reversed this finding. Macrophages transfected with Akt siRNA showed considerably less active Rac1 compared with cells transfected with scrambled siRNA, which was quantified by densitometry of immunoblots from three independent experiments (Fig. 2*E*). Akt siRNA effectively knocked down Akt expression (Fig. 2*E*, *inset*). These observations suggest that Akt expression specifically modulates Rac1 activity in macrophages.

Because Akt increased Rac1 activity and prior data show that Rac1 is primarily localized in the mitochondria of activated alveolar macrophages (24), we asked whether Akt also modulated Rac1 mitochondrial import. Rac1 expression was dramatically altered in the mitochondrial fraction of macrophages

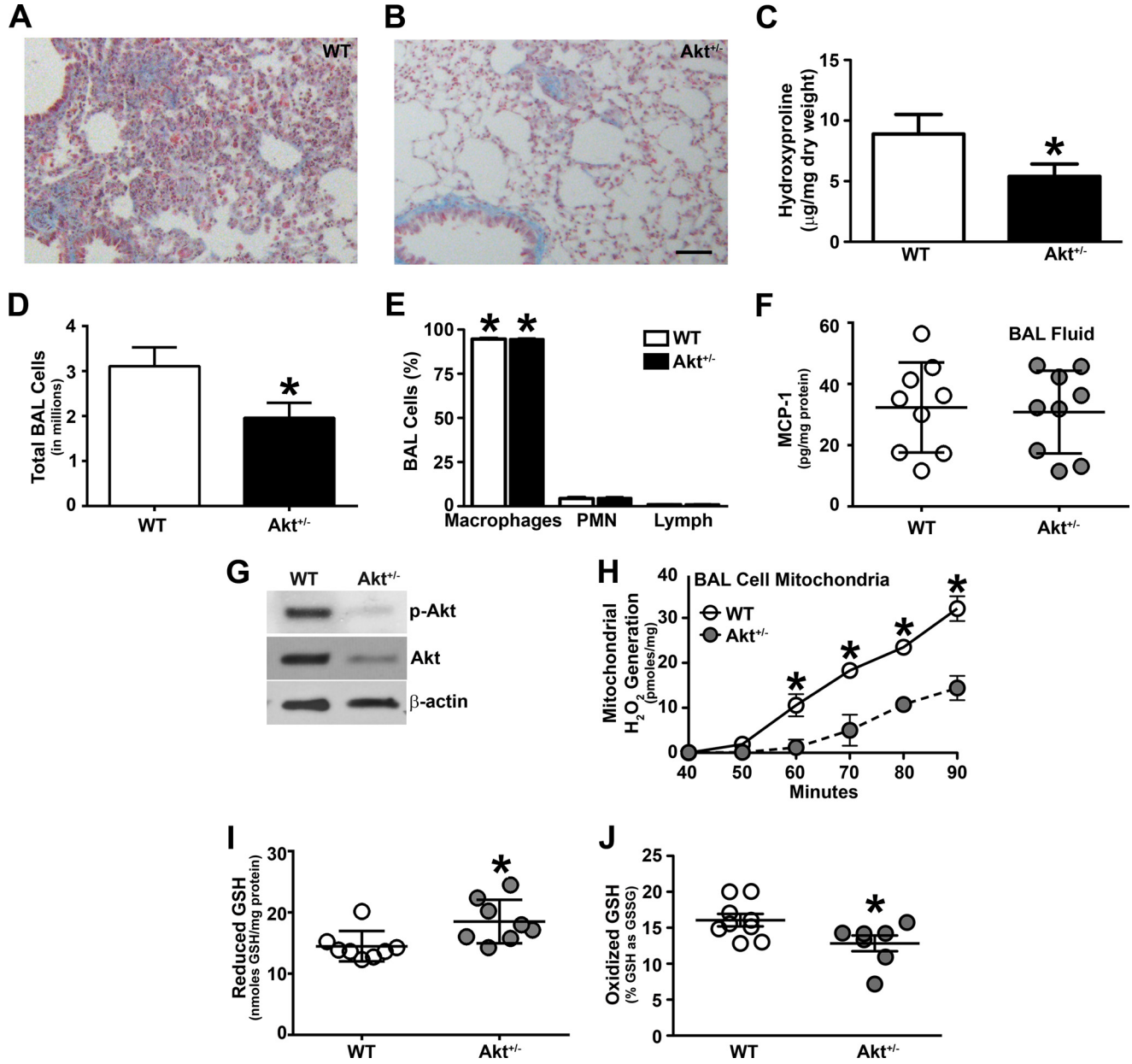

FIGURE 1. **Akt-deficient mice are protected from pulmonary fibrosis.** WT and $Akt^{+/-}$ mice were exposed to 125 μg of chrysotile intratracheally. 21 days later, lungs from WT (*A*) and $Akt^{+/-}$ (*B*) mice were removed and processed for collagen deposition using Masson's trichome staining. Representative micrographs from 1 of 10 mice are shown. *Bar*, 100 μm for both *A* and *B*. *C*, hydroxyproline assay of lungs removed from WT and $Akt^{+/-}$ mice after chrysotile exposure (WT, $n = 8$; $Akt^{+/-}$, $n = 7$). *, $p = 0.043$ *versus* WT. *D*, total number of BAL cells was counted in WT ($n = 10$) and $Akt^{+/-}$ ($n = 10$) mice after chrysotile exposure. *, $p = 0.040$ *versus* WT. *E*, cell differential was determined using Wright-Giemsa stain from BAL performed in WT and $Akt^{+/-}$ after chrysotile exposure (WT, $n = 10$; $Akt^{+/-}$, $n = 10$). *, $p < 0.001$ *versus* polymorphonuclear (*PMN*) cells and lymphs. *F*, MCP-1 levels were measured in BAL fluid from WT ($n = 9$) and $Akt^{+/-}$ ($n = 9$) mice after chrysotile exposure. *G*, macrophages isolated from WT and $Akt^{+/-}$ mice were subjected to immunoblot analysis. *H*, measurement of alveolar macrophage H_2O_2 was performed in isolated mitochondria from BAL cells (WT, $n = 6$; $Akt^{+/-}$, $n = 6$). *, $p = 0.0118$ *versus* $Akt^{+/-}$. Lungs were removed and homogenized for the glutathione assay. *I*, reduced GSH levels in WT ($n = 8$) and $Akt^{+/-}$ ($n = 8$) mice. *, $p = 0.019$ *versus* WT. *J*, total GSH in disulfide form was expressed as the percentage of GSH as GSSG in WT ($n = 9$) and $Akt^{+/-}$ ($n = 7$) mice. *, $p = 0.017$ *versus* WT. *Error bars*, S.D.

with activation of Akt (Fig. 2*F*). The PI3K inhibitor abrogated Rac1 mitochondrial expression, whereas overexpression of Akt greatly increased Rac1 localization. Consequently, Rac1 expression was significantly decreased in the cytoplasmic fraction of cells expressing Akt (Fig. 2*G*), suggesting that Akt, in part, mediates the import of Rac1 from the cytoplasm to the mitochondria. Rac1 activity was also increased in the mitochondrial fraction of macrophages expressing Akt, and LY-294,200 treatment significantly reduced Rac1 activity (Fig. 2*H*). These data indicate that Akt induces Rac1 localization and activity specifically within the mitochondria of macrophages.

Akt Modulates the Mevalonate Pathway and Regulates Rac1 Geranylgeranylation—The mevalonate pathway is involved in multiple cellular processes by converting mevalonate into sterol isoprenoids. The C-terminal cysteine residue in Rac1, Cys^{189}, is modified by geranylgeranylation and is also necessary for import of the protein into the mitochondria (24, 44). Geranylgeranylation is a post-translational lipid modification that

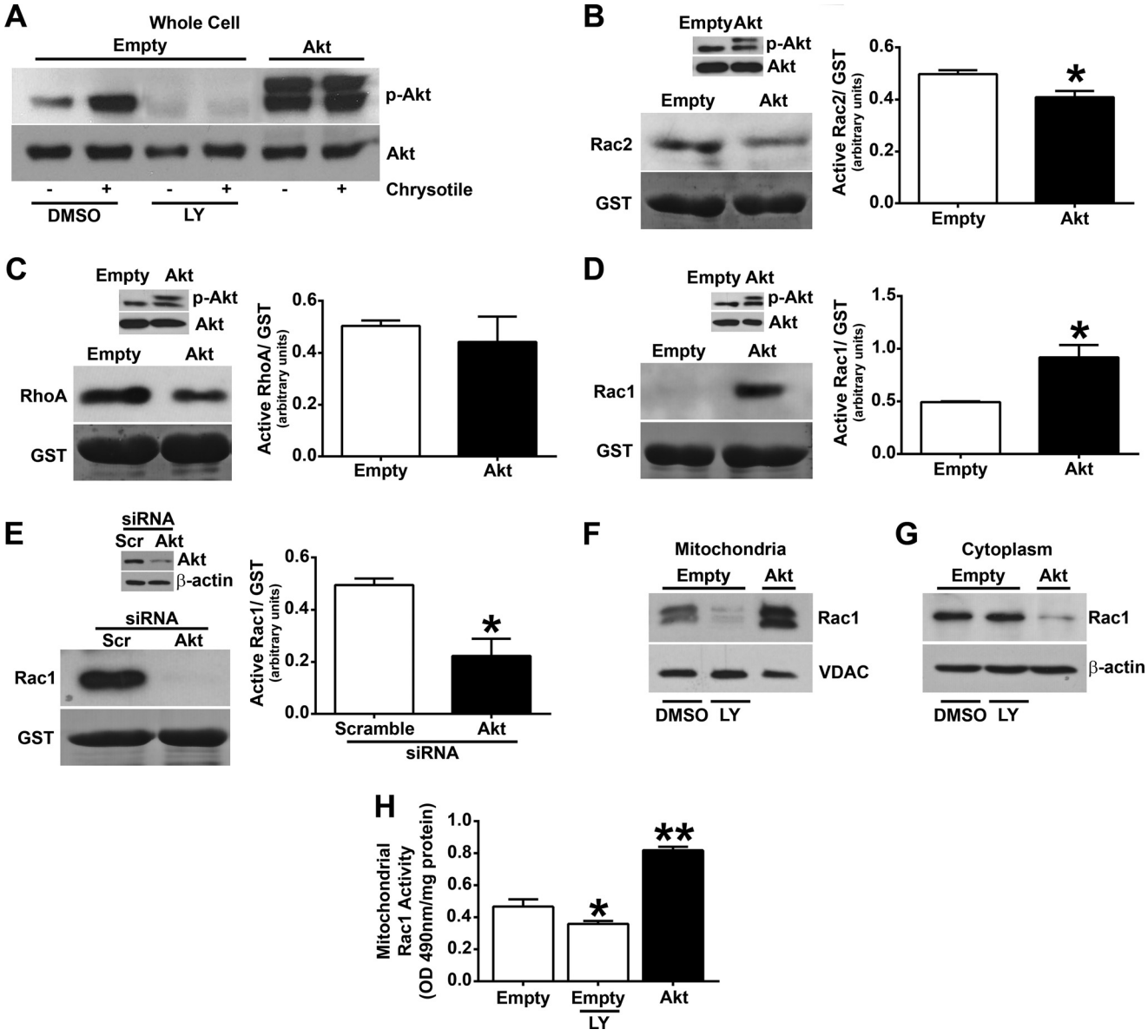

FIGURE 2. **Akt specifically regulates Rac1 activity.** *A*, macrophages were transiently transfected with either an empty or a constitutively active Akt (*Akt*) vector. Cells were incubated with 50 μM LY-294002 (*LY*) or vehicle (DMSO) for 60 min and exposed to chrysotile (10 μg/cm^2) for 30 min. Whole cells were isolated, and immunoblot analysis was performed. Macrophages expressing Akt were analyzed for activation of Rac2 (*B*), RhoA (*C*), and Rac1 (*D*) using a pull-down assay and quantified by densitometry from three independent experiments. *, $p < 0.001$ *versus* empty. *Inset*, overexpression of Akt was confirmed by immunoblot analysis. *E*, macrophages were transfected with scrambled (*Scr*) or Akt siRNA, and Rac1 activity was determined as described above. *Inset*, knockdown of Akt was confirmed by immunoblot analysis. Macrophages expressing empty or Akt were incubated with 50 μM LY-294,200 hydrochloride or vehicle for 60 min. Mitochondrial (*F*) or cytoplasmic (*G*) fractions were isolated, and immunoblot analysis was performed. *H*, active Rac1 was determined in the mitochondrial fraction by the G-LISA kit in cells expressing empty vector or Akt ($n = 9$). *, $p = 0.0132$ *versus* empty; **, $p < 0.0001$ *versus* empty. *Error bars*, S.D.

involves the covalent attachment of geranylgeranyl moieties to C-terminal cysteine residues and is required for Rac1 activation, interaction with other proteins, and mitochondrial import (24, 44). Because Akt specifically regulates Rac1 mitochondrial translocation and activation, we determined whether Akt promotes geranylgeranylation of Rac1. Macrophages were treated with DGBP, a competitive inhibitor of geranylgeranyl diphosphate synthase, the enzyme that catalyzes the formation of geranylgeranyl diphosphate (GGDP). GGDP provides the lipid moiety for the post-translational modification of Rho GTPase proteins, including Rac1 (45). To confirm that DGBP abrogated geranylgeranylation, an immunoblot analysis for Rap 1A, which only recognizes non-geranylgeranylated Rap 1A and is indicative of reduced GGDP levels, showed that DGBP inhibited geranylgeranylation in macrophages expressing the empty vector (Fig. 3*A*). Overexpression of Akt revealed less non-geranylgeranylated Rap 1A expression in the presence of DGBP than in the cells expressing the empty vector, suggesting the presence of higher amounts of geranylgeranylated Rap 1A and increased GGDP levels in cells overexpressing Akt.

To further evaluate the role of Akt regulating Rac1 geranylgeranylation, we determined the prenylation status of Rac1 in cells overexpressing Akt. Lysates were separated into aqueous (hydrophilic) and detergent (hydrophobic) phases with the aqueous fraction containing non-prenylated proteins, whereas the prenylated proteins were retained in the detergent fraction.

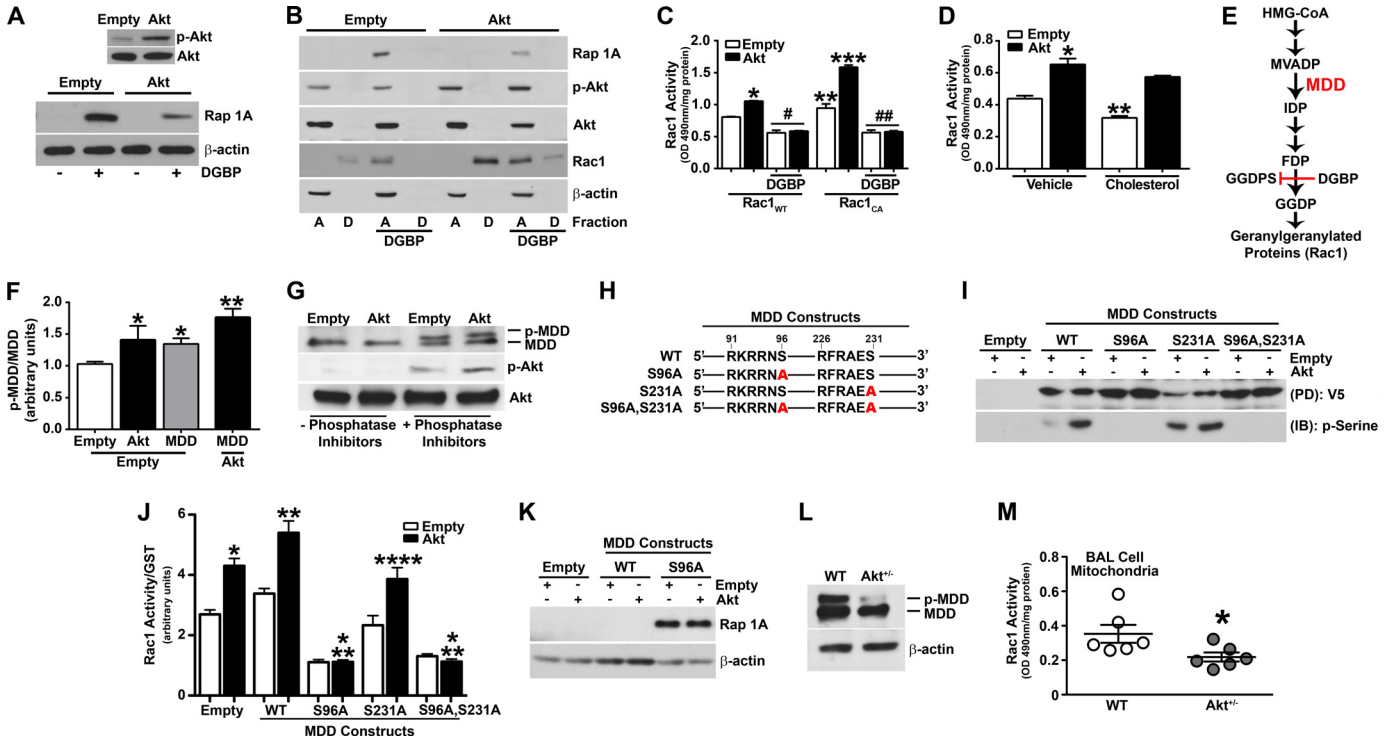

FIGURE 3. **Akt phosphorylates MDD and regulates Rac1 geranylgeranylation.** *A*, macrophages expressing empty or Akt vectors were incubated with 10 μM DGBP or vehicle (water) for 16 h and analyzed by immunoblot analysis for Rap 1A in whole cell lysates. *Inset*, overexpression of Akt was verified by immunoblot analysis. *B*, macrophages expressing empty vector or Akt were incubated with DGBP or vehicle and fractionated into aqueous (*A*) or detergent (*D*) phases. Lysates were subjected to immunoblot analysis. *C*, Rac1 activity was determined in macrophages overexpressing $Rac1_{WT}$ or $Rac1_{CA}$ and co-expressing empty vector or Akt. Macrophages were incubated with DGBP or vehicle ($n = 3$). *, $p < 0.0001$ *versus* $Rac1_{WT}$ (empty); **, $p = 0.0029$ *versus* $Rac1_{WT}$ (empty); ***, $p < 0.0001$ *versus* $Rac1_{CA}$ (empty); #, $p < 0.0001$ *versus* $Rac1_{WT}$ (empty); ##, $p < 0.0001$ *versus* $Rac1_{CA}$ (empty). *D*, Rac1 activity in macrophages overexpressing empty or Akt and treated with vehicle (ethanol) or 100 μM cholesterol for 24 h ($n = 3$). *, $p < 0.0001$ *versus* empty (vehicle); **, $p = 0.0008$ *versus* empty (vehicle). *E*, *schematic diagram* of the mevalonate pathway. Highlighted are MDD and DGBP, which inhibits geranylgeranyl diphosphate synthase (*GGDPS*). *HMG-CoA*, 3-hydroxy-3-methylglutaryl coenzyme A; *MVADP*, mevalonate 5-diphosphate; *IDP*, isopentenyl 5-diphosphate; *FDP*, farnesyl diphosphate; *GGDP*, geranylgeranyl diphosphate. *F*, macrophages transfected with either empty vector or Akt in combination with either empty vector or an MDD vector were subjected to SDS-PAGE (4–15% gradient gel). Immunoblot analysis for phospho-MDD and phospho-Akt was quantified by densitometry ($n = 3$). *, $p < 0.0304$ *versus* empty (empty); **, $p = 0.0147$ *versus* Akt (empty). *G*, cells expressing empty or Akt vectors were lysed in the presence or absence of phosphatase inhibitors. Lysates were subjected to SDS-PAGE (4–15% gradient gel) and immunoblot analysis. *H*, *schematic diagram* of full-length MDD_{WT} construct and MDD constructs with mutations (Ser (*S*) → Ala (*A*)) at potential Akt phosphorylation sites. *I*, macrophages were transfected with empty or Akt vectors and either MDD-V5-His_{WT}, MDD-V5-His_{S96A}, MDD-V5-His_{S231A}, or MDD-V5-$His_{S96A,S231A}$. Lysates were subjected to His pull-down and immunoblot analysis for Ser(P). *J*, Rac1 activity was determined in macrophages expressing empty or MDD constructs using a pull-down assay ($n = 4$). *, $p < 0.0001$ *versus* empty; **, $p < 0.0001$ *versus* MDD_{WT} (empty); ***, $p < 0.0001$ *versus* empty and *versus* MDD_{WT} (empty); ****, $p < 0.001$ *versus* MDD_{S231A} (empty). *K*, immunoblot analysis of macrophages transfected with either empty or Akt vectors in combination with either MDD_{WT} or MDD_{S96A}. *L*, immunoblot analysis of macrophages isolated from WT and $Akt^{+/-}$ mice. *M*, Rac1 activity in mitochondria isolated from BAL cells from WT ($n = 6$) and $Akt^{+/-}$ ($n = 6$) mice. *, $p = 0.049$ *versus* WT. *Error bars*, S.D.

Cells overexpressing Akt showed increased Rac1 expression in the detergent fraction compared with macrophages expressing the empty vector (Fig. 3*B*). DGBP treatment shifted Rac1 expression to the aqueous phase, signifying an impairment of Rac1 geranylgeranylation, which was verified by the expression of non-geranylgeranylated Rap 1A in the aqueous fraction. Unlike cells expressing the empty vector, Rac1 was present in the detergent fraction of cells overexpressing Akt after DGBP treatment, indicating an increase in activation of the mevalonate pathway by Akt. A reduction of non-geranylgeranylated Rap 1A expression was seen in cells overexpressing Akt and treated with DGBP, suggesting the presence of higher amounts of geranylgeranylated Rap 1A compared with cells expressing the empty vector. These data suggest that Akt modulates the mevalonate pathway, which results in the geranylgeranylation of Rac1.

Because DGBP treatment impaired Rac1 geranylgeranylation, we determined whether Rac1 activity was also decreased. DGBP treatment significantly reduced Rac1 activity in macrophages overexpressing a wild-type Rac1 ($Rac1_{WT}$) and in cells co-expressing Akt and $Rac1_{WT}$ (Fig. 3*C*). Macrophages transfected with a constitutively active Rac1 ($Rac1_{CA}$) expression vector had increased Rac1 activity compared with cells expressing $Rac1_{WT}$, and Rac1 activity was greatly enhanced in cells co-expressing $Rac1_{CA}$ and Akt. DGBP treatment of these cells again significantly reduced Rac1 activity (Fig. 3*C*). Examination of the constitutively active Rac1 plasmid revealed the presence of a C-terminal CAA*X* motif, indicating that although Rac1 is constitutively active through a substitution of leucine for glutamine at amino acid 61, the protein still needs to be geranylgeranylated for its activation.

Because the mevalonate pathway regulates cholesterol production and Akt influences Rac1 geranylgeranylation, we determined whether the addition of exogenous cholesterol altered Rac1 activity in macrophages overexpressing Akt. The exogenous addition of cholesterol significantly decreased Rac1 activity in control cells and had no effect on the activity of Rac1 in Akt-expressing cells (Fig. 3*D*). These data suggest that choles-

terol production is not an end product of the mevalonate pathway relative to Akt.

To investigate the mechanism by which the serine/threonine kinase, Akt, induces Rac1 geranylgeranylation, each enzyme within the mevalonate pathway was analyzed for a minimal consensus site(s), Arg-Xaa-Arg-Xaa-Xaa-Ser/Thr, required for Akt phosphorylation. MDD is the only enzyme in the pathway that contained potential Akt phosphorylation sites (Fig. 3*E*). To determine whether Akt directly phosphorylates MDD, macrophages were co-transfected with empty vector and either constitutively active Akt or full-length MDD, and lysates were analyzed using a gradient SDS-polyacrylamide gel to facilitate better separation of similar sized proteins. There was a shift in MDD in cells expressing Akt, suggesting phosphorylation, and it was greatly increased in cells overexpressing Akt and MDD, as verified by densitometry from three independent experiments (Fig. 3*F*). To further verify these findings, macrophages were harvested in the presence or absence of lysis buffer containing phosphatase inhibitors. Macrophages overexpressing Akt that were lysed in the presence of phosphatase inhibitors showed an increase in the phosphorylation of MDD (Fig. 3*G*). In contrast, phosphorylated MDD was not present in cells lysed in a buffer without phosphatase inhibitors. This method was verified by the absence of active Akt in macrophages overexpressing Akt that were lysed in buffer without phosphatase inhibitors. These observations suggest for the first time that Akt modulates the mevalonate pathway by phosphorylating MDD.

Because MDD contains two consensus sites for phosphorylation by Akt, MDD constructs were generated with mutations in either Ser^{96} (MDD-V5-His_{S96A}) or Ser^{231} (MDD-V5-His_{S231A}) as well as a construct containing mutations at both serine residues (MDD-V5-$His_{S96A,S231A}$) (Fig. 3*H*). To determine the specific MDD residue that is phosphorylated by Akt, macrophages were co-transfected with an empty or constitutively active Akt vector and either MDD_{WT}, MDD_{S96A}, MDD_{S231A}, or $MDD_{S96A,S231A}$. Macrophage lysates were subjected to His pull-down, and an immunoblot analysis for Ser(P) was performed. Akt overexpression in cells expressing MDD_{WT} had increased Ser(P) (Fig. 3*I*). This was also seen in cells expressing MDD_{S231A}. In contrast, cells expressing MDD_{S96A} and $MDD_{S96A,S231A}$ constructs showed an absence of Ser(P) in the presence of Akt overexpression. These observations indicate that Akt phosphorylates MDD at Ser^{96}.

Because Akt phosphorylated MDD at the Ser^{96} residue, we next determined whether Rac1 activity was modulated by MDD phosphorylation. Rac1 activity was significantly increased in cells overexpressing Akt and was further induced when Akt and MDD_{WT} were co-expressed (Fig. 3*J*). However, cells expressing MDD_{S96A} had a significant reduction of Rac1 activity that was below control levels. Rac1 activity was similarly reduced in macrophages expressing $MDD_{S96A,S231A}$, whereas the activity with the MDD_{S231A} vector was similar to cells expressing the empty vector. These data suggest that Akt regulates Rac1 activity by directly phosphorylating MDD at Ser^{96}, which augments Rac1 geranylgeranylation. The impairment of geranylgeranylation was verified by an immunoblot analysis of Rap 1A, which indicates a reduction in GGDP, in macrophages transfected with MDD_{S96A} (Fig. 3*K*). These data confirm that phosphorylation of MDD by Akt regulates the prenylation status and activity of Rac1.

To determine the biological relevance of MDD phosphorylation, macrophages were isolated from WT and $Akt^{+/-}$ mice and subjected to analysis using a SDS-PAGE gradient gel. Phosphorylation of MDD was detected in WT mice, whereas MDD phosphorylation was absent in macrophages isolated from $Akt^{+/-}$ mice (Fig. 3*L*). Because Akt-deficient mice had decreased activation of Akt and reduced phosphorylated MDD expression, we verified that Akt and phospho-MDD regulated Rac1 activity *in vivo*. BAL was performed on WT and $Akt^{+/-}$ mice after chrysotile exposure. Mitochondria were isolated, and Rac1 activity was determined. Alveolar macrophages from $Akt^{+/-}$ mice had a significant reduction in mitochondrial Rac1 activity compared with WT mice (Fig. 3*M*). These data suggest that Akt regulates Rac1 activation by phosphorylating MDD *in vitro* and *in vivo*.

Rac1 Is Required for Akt-induced Mitochondrial Oxidative Stress—Because Rac1 activation is linked to mitochondrial oxidative stress (24, 34), we determined whether Akt regulated the ability of Rac1 to induce mitochondrial ROS. Overexpression of Akt increased mitochondrial H_2O_2 levels significantly more than in cells expressing the empty vector (Fig. 4*A*). When both $Rac1_{WT}$ and Akt were overexpressed, an augmented effect was seen. Mitochondrial H_2O_2 was significantly induced compared with overexpression of either vector alone.

Complex III is a major source of ROS generation in mitochondria. We determined if knockdown of Complex III regulated Rac1-induced mitochondrial H_2O_2 generation. Macrophages were transfected with an empty or $Rac1_{WT}$ vector in combination with either scrambled or Rieske siRNA, an iron-sulfur protein component of Complex III. Overexpression of Rac1 increased mitochondrial H_2O_2 production in macrophages transfected with $Rac1_{WT}$ and scrambled siRNA (Fig. 4*B*). In contrast, mitochondrial H_2O_2 generation was completely abrogated below control levels in cells transfected with Rieske siRNA. Overexpression of $Rac1_{WT}$ had no significant effect on restoring H_2O_2 levels in cells also expressing Rieske siRNA. Knockdown of Rieske was confirmed by immunoblot analysis (Fig. 4*B*, *inset*). These data show that Complex III must be active for Rac1 to induce mitochondrial ROS.

We next determined whether the modulation of mitochondrial H_2O_2 generation by Akt requires Rac1. Overexpression of Akt significantly increased mitochondrial H_2O_2 production in cells expressing the scrambled siRNA (Fig. 4*C*), whereas cells transfected with Rac1 siRNA had a significant reduction in mitochondrial H_2O_2 below control levels. Furthermore, Akt had no effect on H_2O_2 levels in the absence of Rac1. Knockdown of Rac1 was confirmed by immunoblot analysis (Fig. 4*C*, *inset*). Taken together, these data show direct evidence that Akt modulates mitochondrial oxidative stress by regulating mitochondrial Rac1 expression and activity in macrophages.

Because Akt regulates macrophage mitochondrial H_2O_2 production and prior data show that abrogating mitochondrial oxidative stress or administration of catalase attenuates pulmonary fibrosis in chrysotile-exposed mice (39), we investigated whether catalase treatment could regulate Akt-mediated ROS production. Macrophages overexpressing Akt and treated with

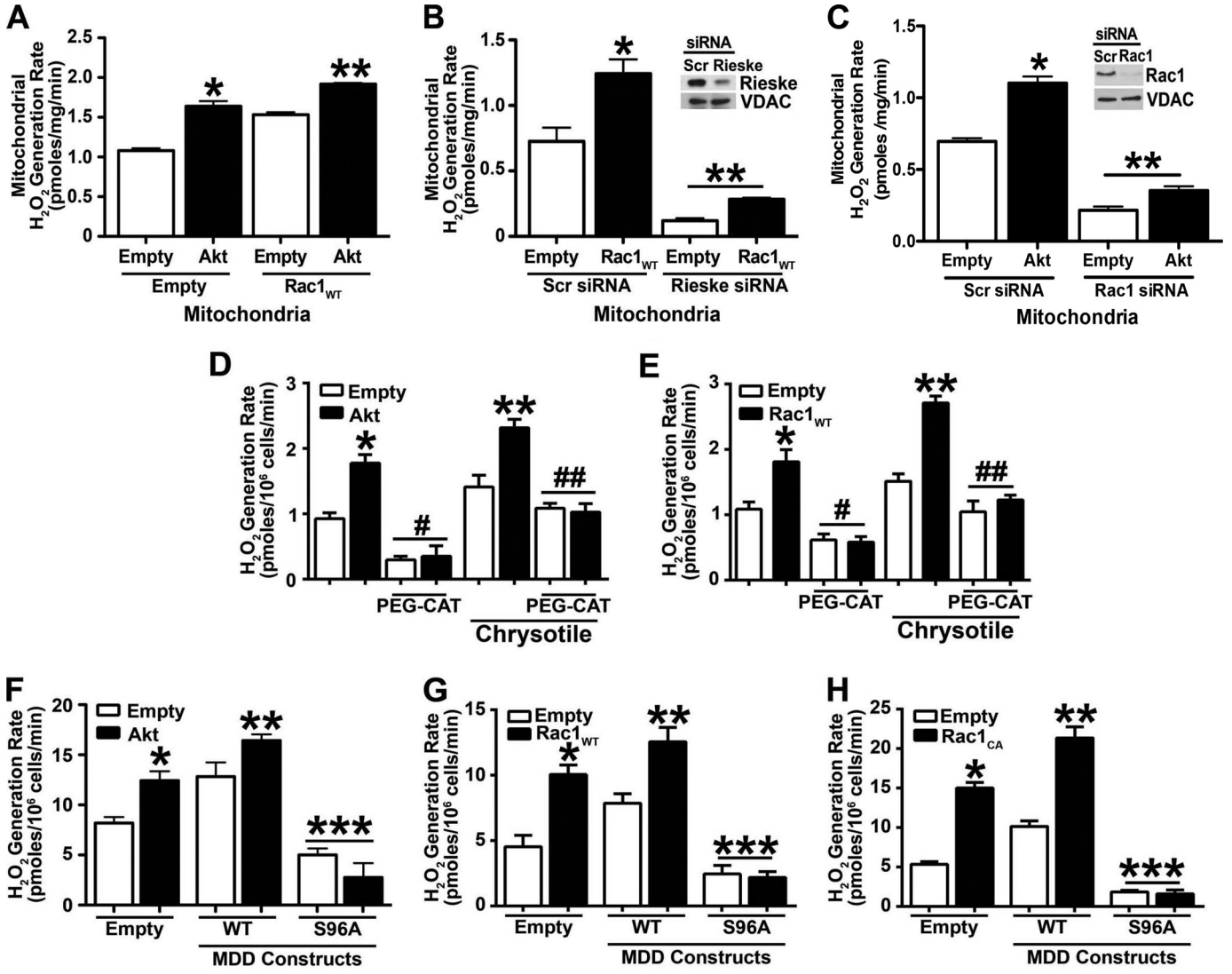

FIGURE 4. **Rac1 is required for Akt-induced mitochondrial oxidative stress.** *A*, macrophages were transfected with empty vector or Akt in combination with either empty or $Rac1_{WT}$ vectors. Mitochondria were isolated, and mitochondrial H_2O_2 was measured ($n = 9$). *, $p < 0.0001$ *versus* empty (empty); **, $p < 0.0001$ *versus* Akt (empty) and *versus* empty (*Rac1*$_{WT}$). *B*, macrophages were transfected with scramble (*Scr*) or Rieske siRNA in combination with empty or $Rac1_{WT}$ vectors. Mitochondria were isolated, and mitochondrial H_2O_2 was measured. *Inset*, Rieske knockdown was verified by immunoblot analysis. $n = 9$. *, $p < 0.0001$ *versus* empty (scramble); **, $p < 0.0001$ *versus* empty (scramble). *C*, macrophages were transfected with scramble or Rac1 siRNA in combination with empty or Akt vectors. Mitochondria were isolated, and mitochondrial H_2O_2 was measured. *Inset*, Rac1 knockdown was verified by immunoblot analysis ($n = 9$). *, $p < 0.001$ *versus* empty (scramble); **, $p < 0.0001$ *versus* empty (scramble). *D*, macrophages were transfected with empty or Akt vectors and treated with catalase (PEG-CAT) for 1 h or pretreated with PEG-CAT and then exposed to chrysotile for 30 min ($n = 8$). *, $p < 0.0001$ *versus* empty; **, $p < 0.001$ *versus* Akt and *versus* empty (chrysotile); #, $p < 0.0001$ *versus* empty; ##, $p < 0.02$ *versus* empty (chrysotile). *E*, macrophages were transfected with empty or $Rac1_{WT}$ vectors and treated with catalase (PEG-CAT) or pretreated with PEG-CAT and then exposed to chrysotile ($n = 8$). *, $p < 0.0001$ *versus* empty; **, $p < 0.001$ *versus* Akt and *versus* empty (chrysotile); #, $p < 0.0003$ *versus* empty; ##, $p < 0.001$ *versus* empty (chrysotile). *F*, macrophages were transfected with empty or Akt vectors and either MDD_{WT} or MDD_{S96A}. H_2O_2 production was measured ($n = 9$). *, $p = 0.031$ *versus* empty (empty); **, $p < 0.035$ *versus* MDD_{WT} (empty); ***, $p < 0.004$ *versus* empty (empty). *G*, macrophages were transfected with empty or $Rac1_{WT}$ vectors and either MDD_{WT} or MDD_{S96A}. H_2O_2 production was measured ($n = 9$). *, $p < 0.014$ *versus* empty (empty); **, $p < 0.0027$ *versus* $Rac1_{WT}$ (empty) and *versus* MDD_{WT} (empty); ***, $p < 0.004$ *versus* empty (empty). *H*, macrophages were transfected with empty or $Rac1_{CA}$ vectors and either MDD_{WT} or MDD_{S96A}. H_2O_2 production was measured ($n = 9$). *, $p < 0.0001$ *versus* empty (empty); **, $p < 0.0001$ *versus* $Rac1_{CA}$ (empty) and *versus* MDD_{WT} (empty); ***, $p < 0.00014$ *versus* empty (empty). *Error bars*, S.D.

PEG-CAT had a significant reduction in H_2O_2 generation compared with controls (Fig. 4*D*). Chrysotile treatment increased ROS production in macrophages expressing the empty vector as well as in macrophages overexpressing Akt. PEG-CAT-reduced H_2O_2 generation was near control levels in cells exposed to chrysotile. Similar findings were seen in macrophages overexpressing $Rac1_{WT}$ (Fig. 4*E*).

Because Akt regulates Rac1 geranylgeranylation by modulating MDD phosphorylation at Ser^{96}, we determined whether MDD overexpression altered H_2O_2 generation. ROS generation was significantly induced in macrophages co-expressing Akt and MDD_{WT} (Fig. 4*F*). In contrast, the MDD_{S96A} construct showed minimal H_2O_2 production that was dramatically reduced compared with cells expressing the empty vector. Because MDD overexpression induced H_2O_2 production, we determined whether the ROS production was mediated through Rac1. Macrophages co-expressing $Rac1_{WT}$ and MDD_{WT} showed a significant induction of H_2O_2 generation compared with cells expressing the empty vector, and the mutant MDD_{S96A} reduced ROS below control levels (Fig. 4*G*).

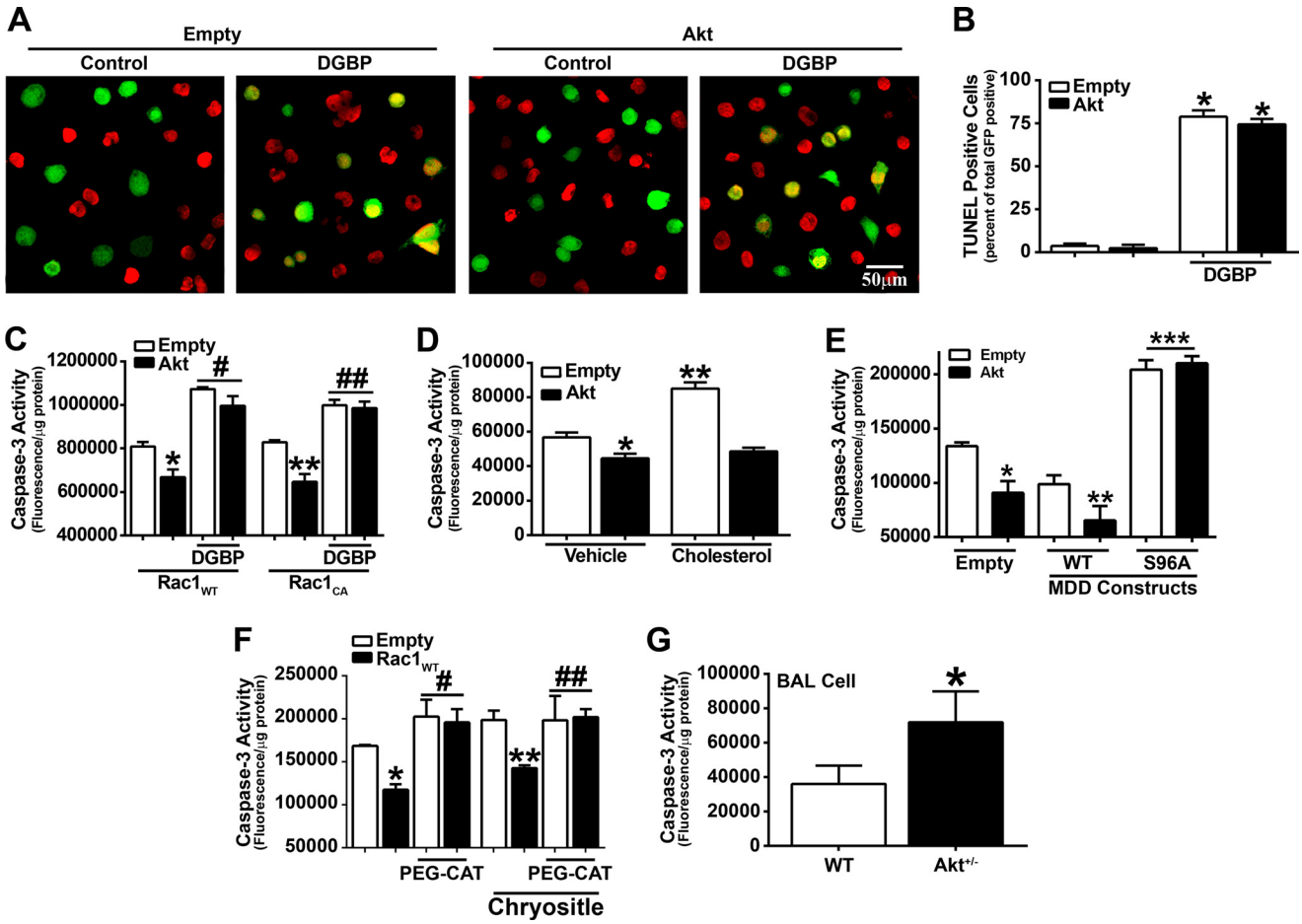

FIGURE 5. **Akt mediates macrophage cell survival.** *A*, representative images of apoptotic nuclear TUNEL staining in macrophages expressing empty and phMGFP-empty vectors or Akt and phMGFP-empty vectors. Cells were treated with 10 μM DGBP or vehicle for 16 h. *B*, quantitative analysis of *A* expressed as a ratio of number of TUNEL-positive and GFP-positive cells to the total number of GFP-positive cells. Counts were conducted on five different fields within each group. *, $p < 0.001$ *versus* empty and *versus* Akt. *C*, caspase-3 activity was determined in macrophages overexpressing $Rac1_{WT}$ or $Rac1_{CA}$ and co-expressing empty or Akt. Macrophages were incubated with DGBP or vehicle ($n = 8$). *, $p < 0.0001$ *versus* $Rac1_{WT}$ (*Empty*); **, $p < 0.0001$ *versus* $Rac1_{CA}$ (*Empty*); #, $p < 0.0001$ *versus* $Rac1_{WT}$ (*Empty*); ## $p < 0.0001$ *versus* $Rac1_{CA}$ (*Empty*). *D*, macrophages expressing Akt were analyzed for caspase-3 activity in cells incubated in vehicle (ethanol) or 100 μM cholesterol for 24 h. $n = 8$. *, $p < 0.0001$ *versus* empty (*Vehicle*); **, $p = 0.0008$ *versus* empty (*Vehicle*). *E*, caspase-3 activity was measured in macrophages expressing empty or Akt vectors and either MDD_{WT} or MDD_{S96A}. $n = 8$. *, $p < 0.0001$ *versus* empty (*Empty*); **, $p < 0.0001$ *versus* MDD_{WT} (*Empty*); ***, $p < 0.0001$ *versus* MDD_{WT} (*Empty*). *F*, macrophages were transfected with empty or $Rac1_{WT}$ vectors and treated with catalase (PEG-CAT) for 1 h or pretreated with PEG-CAT and then exposed to chrysotile for 30 min ($n = 8$). *, $p < 0.0001$ *versus* empty; **, $p < 0.0425$ *versus* $Rac1_{WT}$ (*Vehicle*) and *versus* empty (*Chrysotile*); #, $p < 0.0376$ *versus* empty; ##, $p < 0.0174$ *versus* empty. *G*, caspase-3 activity was analyzed in BAL cells from WT ($n = 4$) and $Akt^{+/-}$ ($n = 4$) mice. *, $p < 0.0406$ *versus* WT. *Error bars*, S.D.

Next we determined whether a similar effect could be seen in cells expressing $Rac1_{CA}$. Macrophages expressing $Rac1_{CA}$ showed greater H_2O_2 production than cells expressing the empty vector, and MDD_{WT} increased ROS generation further. Although cells expressing $Rac1_{CA}$ had a greater -fold increase in H_2O_2 than the $Rac1_{WT}$, cells co-expressing $Rac1_{CA}$ and the mutant MDD_{S96A} had reduced ROS below control levels, confirming that MDD is required for geranylgeranylation (Fig. 4*H*). In aggregate, these data indicate that Akt-mediated phosphorylation of MDD augments Rac1 activation by geranylgeranylation and is required for Rac1-mediated mitochondrial oxidative stress.

Akt Mediates Cell Survival—Because Akt is activated in many human diseases and both Akt and the mevalonate pathway have a significant role in cell survival (10–12, 20, 21, 46), we determined the relationship of macrophage survival and Akt with pulmonary fibrosis. Using TUNEL staining to detect DNA fragmentation, DGBP treatment induced apoptosis in macrophages expressing the empty vector, whereas overexpression of Akt had no significant effect on reducing DGBP-mediated apoptosis (Fig. 5*A*). These results were quantified by counting the total number of GFP- and TUNEL-positive cells relative to GFP-positive cells (Fig. 5*B*). These results suggest that Akt regulates apoptosis by modulating the mevalonate pathway.

We next determined whether Akt influenced macrophage cell survival and required Rac1. Macrophages co-expressing Akt and $Rac1_{WT}$ or Akt and $Rac1_{CA}$ had a significant reduction in caspase-3 activity relative to cells expressing the empty vector (Fig. 5*C*). Because DGBP treatment impaired Rac1 geranylgeranylation and activation, we investigated whether DGBP treatment altered caspase-3. Macrophages treated with DGBP had a significant increase in caspase-3 activity in all conditions (Fig. 5*C*). These data provide additional evidence that Akt regulates apoptosis by modulating the mevalonate pathway, and impairment of geranylgeranylation with DGBP treatment induces apoptosis.

Because cholesterol is one product of the mevalonate pathway and the exogenous addition of cholesterol significantly decreased active Rac1, we determined whether cholesterol altered cell survival. Exogenous cholesterol induced apoptosis mediated through caspase-3 in control cells; however, overexpression of Akt significantly reduced the cholesterol-mediated apoptosis to levels similar to those of untreated macrophages expressing Akt (Fig. 5*D*). Unlike chrysotile, Akt does not require overexpression of Rac1 to modulate cholesterol-induced apoptosis.

To directly determine whether Akt mediated cell survival via the mevalonate pathway, macrophages were transfected with MDD constructs, and caspase-3 activity was analyzed. Overexpression of MDD_{WT} significantly reduced caspase-3 activity in cells transfected with empty vector or Akt, whereas Akt had no effect on altering active caspase-3 in cells expressing MDD_{S96A} (Fig. 5*E*). Taken together, disruption of the mevalonate pathway induces macrophage apoptosis.

Because administration of PEG-CAT decreased H_2O_2 generation in macrophages overexpressing Akt or $Rac1_{WT}$, we determined whether catalase modulated macrophage apoptosis. PEG-CAT-treated macrophages expressing empty vector or $Rac1_{WT}$ had a significant increase in caspase-3 activity compared with controls. Chrysotile exposure of cells overexpressing $Rac1_{WT}$ that were pretreated with PEG-CAT had increased caspase-3 activity compared with chrysotile-exposed cells overexpressing $Rac1_{WT}$ treated with vehicle (Fig. 5*F*). PEG-CAT did not alter Akt activation by chrysotile, suggesting that PEG-CAT induces apoptosis by a mechanism other than reducing Akt expression (data not shown). These data validate targeting the Akt signaling pathway to halt the progression of pulmonary fibrosis.

Because $Akt^{+/-}$ mice have decreased active Rac1 in alveolar macrophages, we determined whether the combination of Akt deficiency and decreased Rac1 activity induced apoptosis in alveolar macrophages. WT and $Akt^{+/-}$ mice were exposed to chrysotile, and BAL was performed. BAL cells isolated from $Akt^{+/-}$ mice had a significant increase in caspase-3 activity compared with WT mice (Fig. 5*G*). These data suggest that $Akt^{+/-}$ mice have reduced macrophage survival due to increased apoptosis. Taken together, these data suggest that Akt and Rac1 enhance macrophage survival and lead to the development of a fibrotic phenotype *in vivo*.

Akt Modulates Macrophage M2 Polarization and Expression of TGF-β1—Macrophages play a critical role in the pathogenesis of pulmonary fibrosis, and macrophage plasticity is an important feature in these immune cells. Activated macrophages are defined by two distinct phenotypes, classically activated (M1) and alternatively activated (M2), depending on their response to stimuli. Because fibrosis is associated with a dominant M2 phenotype and Akt has been associated with M2 macrophage polarization (47–49), we investigated the role of Akt in macrophage polarization in our model. Macrophages overexpressing Akt had a significant increase in M2 genes (arginase-1; chitinase-like secretory lectin, Ym1; and TGF-β1), whereas M1 genes (TNF-α and IL-1β) were down-regulated or unchanged (Fig. 6*A*).

Because Akt induced TGF-β1 mRNA expression, we examined whether this was mediated through Rac1. Overexpression of $Rac1_{WT}$ significantly increased TGF-β1 mRNA expression in cells transfected with empty or Akt (Fig. 6*B*). When these cells were exposed to chrysotile, TGF-β1 expression was further induced.

TGF-β1 is a pro-fibrotic growth factor that stimulates collagen synthesis in fibroblasts and myofibroblasts. Previous studies show that mitochondrial ROS are essential for normal TGF-β1-mediated gene expression because inhibition of mitochondrial ROS generation attenuates pro-fibrotic gene expression, including TGF-β1 (35, 50). Because Rac1 and Akt induced TGF-β1 expression, we determined whether Akt also modulated collagen production. Human lung fibroblasts were cultured in conditioned medium from macrophages overexpressing empty or constitutively active Akt expression vectors. Compared with cells exposed to the conditioned medium from the empty vector, fibroblasts incubated with conditioned medium from macrophages overexpressing Akt had increased collagen I production (Fig. 6*C*). Densitometry of the immunoblot analyses from three independent experiments revealed a significant increase in collagen I expression in fibroblasts exposed to conditioned medium from macrophages overexpressing Akt (Fig. 6*C*). Conversely, fibroblasts exposed to conditioned medium from macrophages transfected with Akt siRNA had a significant decrease in collagen I compared with cells exposed to the conditioned medium from macrophages transfected with scrambled siRNA (Fig. 6*D*). Knockdown of Akt by siRNA was confirmed by immunoblot analysis (Fig. 6*D*, *inset*).

To corroborate these observations *in vivo* in a fibrosis model, WT and $Akt^{+/-}$ mice were exposed to chrysotile intratracheally. WT mouse lung fibroblasts were cultured in BAL fluid from WT and $Akt^{+/-}$ mice to measure collagen I production. Fibroblasts incubated with BAL fluid from $Akt^{+/-}$ mice had decreased procollagen and collagen I secretion compared with WT mice (Fig. 6*E*). This was confirmed by densitometry of the immunoblots showing a significant decrease in collagen I expression in fibroblasts incubated with BAL fluid from $Akt^{+/-}$ mice (Fig. 6*E*).

Because Akt modulates the mevalonate pathway by phosphorylation of MDD, we determined whether Akt and MDD induce M2 polarization. Overexpression of MDD_{WT} increased arginase I mRNA expression in cells transfected with empty vector or Akt (Fig. 6*F*). However, cells expressing MDD_{S96A} together with empty vector or Akt had levels of arginase I expression below control levels. These data suggest that Akt and MDD work together to promote cell survival and macrophage M2 polarization.

To determine whether macrophage polarization and pro-fibrotic proteins were altered in $Akt^{+/-}$ mice, TNF-α, Ym1, and TGF-β1 were measured in BAL fluid. $Akt^{+/-}$ mice had significantly less Ym1 and active TGF-β1 in BAL fluid than WT mice (Fig. 6*G*). Taken together, these data suggest that Akt induces a pro-fibrotic environment, in part, by inducing M2 polarization and increasing TGF-β1 production in macrophages. Furthermore, the M2 phenotype has been shown to prolong macrophage cell survival (40, 51–55).

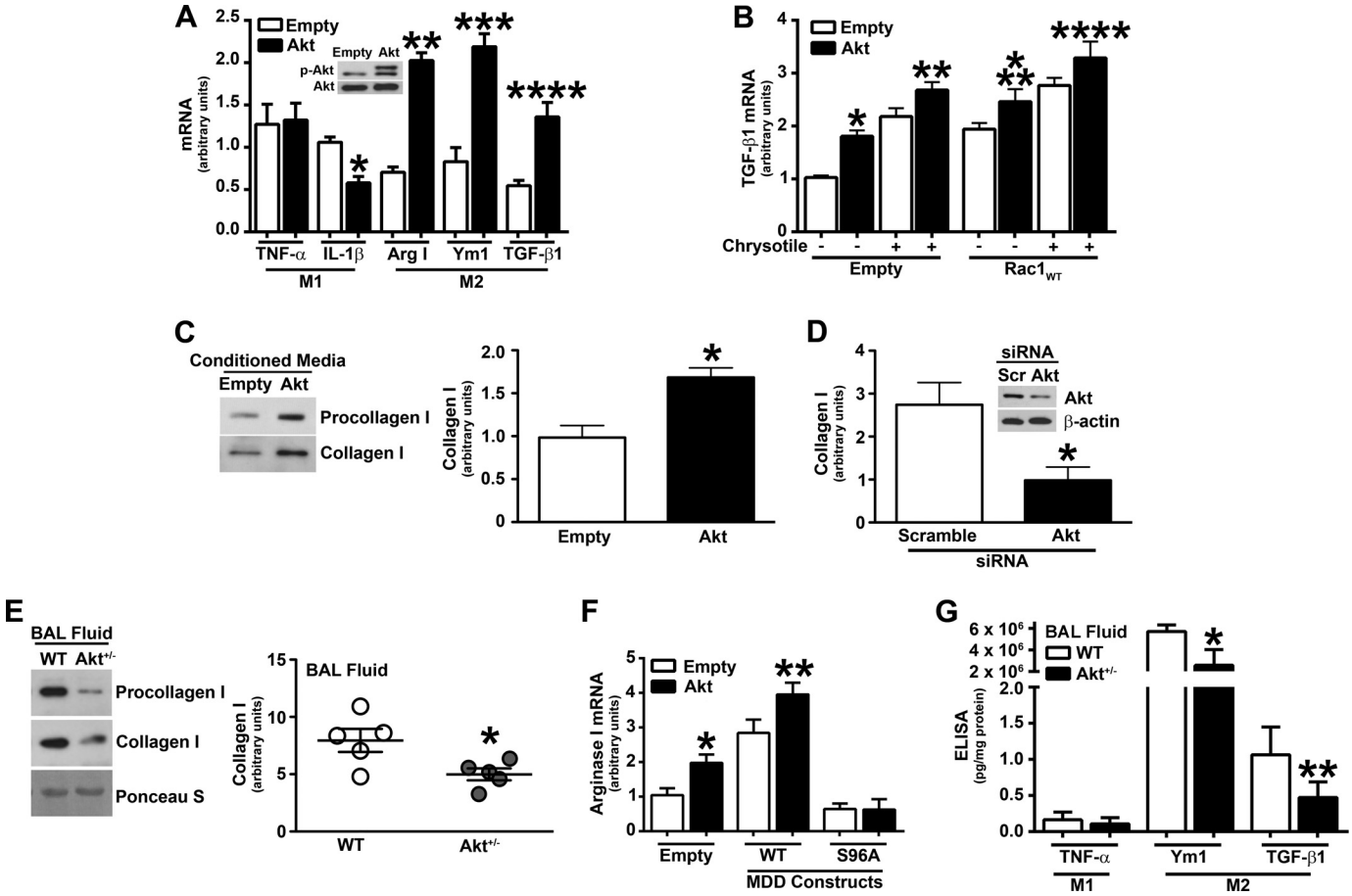

FIGURE 6. **Akt modulates M2 macrophage polarization and TGF-β1 gene expression.** *A*, total RNA was isolated, and mRNA expression was measured by real-time PCR in macrophages expressing empty or Akt vectors. Results show arbitrary units normalized to β-actin mRNA ($n = 9$). *, $p = 0.0011$ *versus* IL-1β empty; **, $p = 0.0036$ *versus* Arg I empty; ***, $p = 0.0027$ *versus* Ym1 empty; ****, $p = 0.0015$ *versus* TGF-β1 empty. *B*, TGF-β mRNA expression was measured in macrophages expressing empty or $Rac1_{WT}$ together with empty or Akt. Results show arbitrary units normalized to hypoxanthine-guanine phosphoribosyltransferase mRNA ($n = 9$). *, $p = 0.0012$ *versus* empty (empty); **, $p = 0.0495$ *versus* empty (empty with chrysotile); ***, $p = 0.0381$ *versus* Rac1 (empty); ****, $p = 0.0381$ *versus* Rac1 (empty with chrysotile). *C*, human lung fibroblasts (HLF-1) were incubated with conditioned medium from macrophages expressing empty or Akt vectors. Shown is immunoblot analysis of procollagen and collagen I from medium. The graph shows densitometry from three independent experiments ($n = 9$). *, $p = 0.009$ *versus* empty. *D*, HLF-1 were incubated with conditioned medium from macrophages expressing scramble (*Scr*) or Akt siRNA. Knockdown of Akt was confirmed by immunoblot analysis (*inset*). Quantification of collagen I expression from three separate experiments by densitometry ($n = 9$). *, $p = 0.022$ *versus* scramble. *E*, mouse lung fibroblasts from WT mice were incubated with BAL fluid from chrysotile exposed WT ($n = 5$) or $Akt^{+/-}$ ($n = 5$) mice. Immunoblot analysis of procollagen and collagen I from medium, which was quantified by densitometry. *, $p = 0.015$ *versus* WT. *F*, arginase I mRNA expression was measured in macrophages expressing empty or Akt together with MDD_{WT} or MDD_{S96A}. Results show arbitrary units normalized to β-actin mRNA. $n = 9$. *, $p = 0.0132$ *versus* empty (empty); **, $p = 0.0156$ *versus* MDD_{WT} (empty). *G*, TNF-α, Ym1, and active TGF-β1 levels were measured in BAL fluid from WT ($n = 9$) and $Akt^{+/-}$ ($n = 10$) mice 21 days after chrysotile exposure. *, $p = 0.0031$ *versus* Ym1 WT; **, $p = 0.0039$ *versus* TGF-β1 WT. *Error bars*, S.D.

Alveolar Macrophages from Patients with Asbestosis Have Increased Akt Activation—Because Akt activation is prevalent in many human cancers, diabetes, and neurological disorders, and increased expression of Akt is associated with some fibrotic diseases (56–58), we determined whether Akt expression was increased in alveolar macrophages obtained from patients with pulmonary fibrosis. The active form of Akt was significantly greater in alveolar macrophages obtained from lungs of patients with asbestosis compared with normal subjects, whereas the expression of total Akt was similar (Fig. 7*A*). Densitometry of the immunoblot analyses from several subjects revealed a 2-fold increase of active Akt in alveolar macrophages of asbestosis patients (Fig. 7*A*). We investigated whether the mevalonate pathway was activated in patients compared with normal subjects. Alveolar macrophages obtained from lungs of patients with asbestosis had significantly greater phosphorylated MDD compared with normal volunteers (Fig. 7*B*). To quantify this difference, the phosphorylated MDD was expressed as ratio to total MDD expression by densitometry of the immunoblot analyses from several subjects (Fig. 7*B*).

To corroborate and extend our *in vitro* data, we determined the activity of several GTPases in alveolar macrophages obtained from lungs of patients with asbestosis and normal subjects. The activity of Rac1 was increased in patients with asbestosis, whereas other prominent GTPase proteins (Rac2 and RhoA) were decreased or not modulated in asbestosis patients (Fig. 7*C*).

Because asbestosis patients have increased active Akt and phospho-MDD expression levels in alveolar macrophages and asbestosis is characterized by enhanced cell proliferation and aberrant collagen deposition, we determined whether alveolar macrophages from asbestosis patients were protected from apoptosis. Active caspase-9 and -3 expression was significantly reduced in asbestosis patients compared with normal subjects

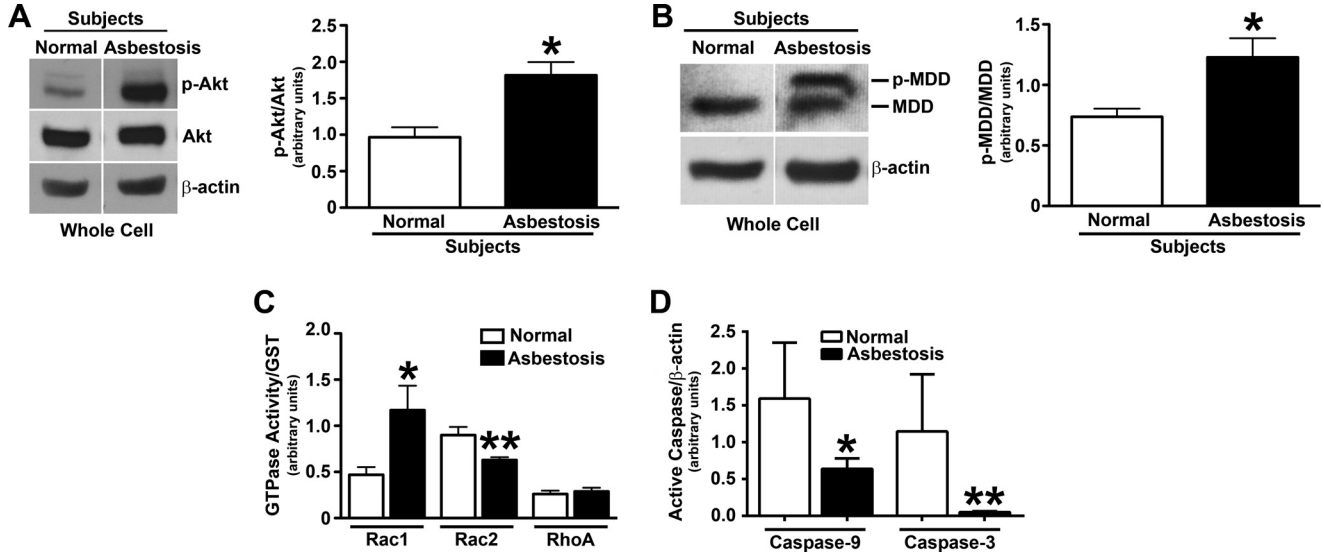

FIGURE 7. **Alveolar macrophages from asbestosis patients have increased Akt activation and cell survival.** Alveolar macrophages were obtained from normal subjects and asbestosis patients. *A*, a representative immunoblot analysis for phospho-Akt in whole cell lysates is shown. A quantitative analysis of phospho-Akt immunoblots normalized to total Akt is shown by densitometry in normal subjects ($n = 4$) and asbestosis patients ($n = 4$). *, $p = 0.0048$ *versus* normal. *B*, a representative immunoblot analysis for phospho-MDD in whole cell lysates subjected to SDS-PAGE (4–15% gradient gel) is shown. A quantitative analysis of phospho-MDD immunoblots normalized to total MDD by densitometry is shown in normal subjects ($n = 4$) and asbestosis patients ($n = 4$). *, $p = 0.014$ *versus* normal. *C*, activity of Rac1, Rac2, and RhoA was measured in whole cell lysates of alveolar macrophages from normal subjects ($n = 4$) and asbestosis patients ($n = 4$) using a pull-down assay. Immunoblots were quantified by densitometry of each GTPase protein relative to GST expression. *, $p = 0.0221$ *versus* Rac1 normal subjects. **, $p = 0.0132$ *versus* Rac2 normal subjects. *D*, immunoblot analysis from normal subjects ($n = 4$) and asbestosis patients ($n = 5$) was quantified by densitometry for active caspase-9 and -3 relative to β-actin. *, $p = 0.0268$ *versus* caspase-9 normal subjects. **, $p = 0.0148$ *versus* caspase-3 normal subjects. *Error bars*, S.D.

(Fig. 7*D*). These data strongly suggest that activation of Akt protects alveolar macrophages from apoptosis by directly increasing flux through the mevalonate pathway. In aggregate, these observations demonstrate that Akt is required for pulmonary fibrosis by directly modulating the post-translational modification of Rac1 in alveolar macrophages. Furthermore, these findings reveal a novel therapeutic target to attenuate the development of fibrosis.

DISCUSSION

The phosphatidylinositol 3-kinase (PI3K) and the key mediator of PI3K signaling, protein kinase B (Akt), play a critical role in multiple cell functions, including cell metabolism, growth, survival, proliferation, and migration, as well as innate immunity and oxidative stress. This wide range of effects is the result of phosphorylation of effector proteins, of which nearly 50 substrates have been described, to inhibit or enhance function (59). The activation of the serine/threonine kinase Akt is altered in human disease, such as diabetes, several neurological diseases, and cancer (8, 9, 60–63). Interestingly, these diseases are often treated by disrupting the mevalonate pathway (20, 21, 64, 65); however, Akt is not known to regulate the mevalonate pathway. Akt has also been associated with the development of fibrosis when activated in hepatocytes *ex vivo* or human lung fibroblasts *in vitro* (10–12). Akt activation in macrophages in the setting of pulmonary fibrosis is, to our knowledge, unknown. In this study, we provide evidence to support the notion that Akt activation enhances macrophage survival by modulating the mevalonate pathway, which uncovers a novel molecular mechanism that mediates a fibrotic phenotype.

The association between Akt and Rac1 is complex and controversial. Some reports indicate that Rac1 is located upstream of Akt and promotes Akt signaling (29, 32, 33). Akt has also been shown to negatively regulate (30, 31) or positively regulate Rac1 activation (28, 66, 67). Besides inhibition of Rac1 binding to GTP by phosphorylation (31), the molecular mechanism by which Akt modulates Rac1 activation has not been described.

The C-terminal cysteine residue (Cys^{189}) of Rac1 is required for activation by geranylgeranylation, a lipidation process common to all Rho GTPases. Geranylgeranylation is necessary for proper cellular localization and activity as well as association with other proteins (24, 44). The GTPase Ras is activated and localized to the plasma membrane after the post-translational addition of farnesyl or geranylgeranyl isoprenoid moieties to its C-terminal cysteine residue. Disrupting the activity of Ras using a farnesyltransferase inhibitor down-regulates the PI3K/Akt pathway, because PI3K is a known downstream substrate of Ras (68). Our data reveal that Akt regulates Rac1 activation by enhancing geranylgeranylation of Rac1, which is required for activation and modulation of mitochondrial ROS generation.

Several pharmaceutical agents have been designed to target enzymes in the mevalonate biosynthetic pathway as therapy for multiple conditions, including hypercholesterolemia, cardiovascular disease (69), osteoporosis (16), Alzheimer disease (70), several infectious diseases (17, 18, 71), and cancer (19). Inhibition of farnesyltransferase, geranylgeranyltransferase I, and geranylgeranyltransferase II, the enzymes responsible for the farnesylation and geranylgeranylation of proteins, decreases cell survival, migration, and proliferation in many cancers (19). A farnesyltransferase inhibitor, FTI-277, is known to decrease Akt-mediated growth factor- and adhesion-dependent survival pathways and induce apoptosis in human cancer cells that overexpress Akt2. This study demonstrates a mechanistic approach

of inhibiting tumor growth by inducing apoptosis through inhibition of the Akt pathway (19). These findings suggest that the post-translational modification of the Rho GTP-binding proteins and Akt do not work in combination to modulate cell survival. In contrast, our observations suggest that Akt augments the geranylgeranylation and activity of Rac1 by regulating the mevalonate pathway to enhance macrophage cell survival.

MDD performs the first committed step in the biosynthesis of isoprenes. The conserved Asp^{302} in MDD is required for catalytic activity (72). Although the Ser^{96} residue is phosphorylated in HeLa cells during mitosis (73), the kinase is not known, and Ser^{96} is not known to be required for activation. MDD, the enzyme responsible for catalyzing the ATP-dependent decarboxylation of mevalonate 5-diphosphate to form isopentenyl 5-diphosphate, has two minimal sequence motifs (Arg-Xaa-Arg-Xaa-Xaa-Ser) for Akt phosphorylation (74). Our data show for the first time that the phosphorylation of MDD at the Ser^{96} residue activates the mevalonate pathway and up-regulates Rac1 by enhancing geranylgeranylation, and Akt triggers this post-translational modification.

Both Akt and the mevalonate pathway are known to increase cell survival (10–12, 20, 21, 46). Macrophages in chronic disease often have increased survival, and the survival is generally associated with disease progression. In fact, conditional macrophage depletion was shown to attenuate liver injury and lung injury *in vivo* (53, 75). Furthermore, phagocytosis of apoptotic cells, which are frequently present in tissue injury, augments cell survival (76). The macrophage phenotype is also associated with survival. Studies have shown that alternatively activated macrophages (M2) promote repair of injured tissue, which prolongs macrophage cell survival (40, 51–55). The current data demonstrate that Akt modulates the mevalonate pathway and that Akt and MDD work in combination to promote M2 polarization and cell survival. Moreover, the current study demonstrates that macrophage survival is associated with a fibrotic phenotype *in vivo*.

Currently, there are no therapeutic measures that can prevent the development of pulmonary fibrosis or halt its progression. Alveolar macrophages play a key role in the pathogenesis of fibrosis by initiating an immune response and by generating high levels of ROS, which have been directly linked to the progression of pulmonary fibrosis (40). Rac1 is an important mediator of mitochondrial H_2O_2 production, and the activation of Rac1 by geranylgeranylation in alveolar macrophages has been shown to be associated with the development of oxidative stress in the lung (24).

Although Rac1-induced oxidative stress has been linked to pulmonary fibrosis, little is known about upstream regulators of this process. Results from this study clearly demonstrate that Akt modulates the geranylgeranylation of Rac1 by phosphorylation of MDD, which controls Rac1 activation and its ability to mediate oxidative stress. The importance of Akt and the mevalonate pathway *in vivo* show that alveolar macrophages from $Akt^{+/-}$ mice have reduced Rac1 activity and ROS generation and undergo apoptosis. More importantly, $Akt^{+/-}$ mice are protected from pulmonary fibrosis. Taken together, our data demonstrate the molecular mechanisms by which Akt and the mevalonate pathway are linked to a fibrotic phenotype in mice. Furthermore, these observations provide a novel therapeutic target for preventing the progression and development of pulmonary fibrosis.

Acknowledgments—We thank Thomas Moninger and the Central Microscopy Research Facilities at the University of Iowa for assistance with confocal microscopy and Jeffrey D. Neighbors and Raymond Hohl (University of Iowa) for generously providing DGBP.

REFERENCES

1. Datta, S. R., Brunet, A., and Greenberg, M. E. (1999) Cellular survival: a play in three Akts. *Genes Dev.* **13,** 2905–2927
2. Zha, J., Harada, H., Yang, E., Jockel, J., and Korsmeyer, S. J. (1996) Serine phosphorylation of death agonist BAD in response to survival factor results in binding to 14-3-3 not BCL-X(L). *Cell* **87,** 619–628
3. Datta, S. R., Dudek, H., Tao, X., Masters, S., Fu, H., Gotoh, Y., and Greenberg, M. E. (1997) Akt phosphorylation of BAD couples survival signals to the cell-intrinsic death machinery. *Cell* **91,** 231–241
4. Cardone, M. H., Roy, N., Stennicke, H. R., Salvesen, G. S., Franke, T. F., Stanbridge, E., Frisch, S., and Reed, J. C. (1998) Regulation of cell death protease caspase-9 by phosphorylation. *Science* **282,** 1318–1321
5. Pommier, Y., Sordet, O., Antony, S., Hayward, R. L., and Kohn, K. W. (2004) Apoptosis defects and chemotherapy resistance: molecular interaction maps and networks. *Oncogene* **23,** 2934–2949
6. Zhou, B. P., Liao, Y., Xia, W., Zou, Y., Spohn, B., and Hung, M. C. (2001) HER-2/neu induces p53 ubiquitination via Akt-mediated MDM2 phosphorylation. *Nat. Cell Biol.* **3,** 973–982
7. Mayo, L. D., and Donner, D. B. (2001) A phosphatidylinositol 3-kinase/Akt pathway promotes translocation of Mdm2 from the cytoplasm to the nucleus. *Proc. Natl. Acad. Sci. U.S.A.* **98,** 11598–11603
8. Cho, H., Mu, J., Kim, J. K., Thorvaldsen, J. L., Chu, Q., Crenshaw, E. B., 3rd, Kaestner, K. H., Bartolomei, M. S., Shulman, G. I., and Birnbaum, M. J. (2001) Insulin resistance and a diabetes mellitus-like syndrome in mice lacking the protein kinase Akt2 (PKB β). *Science* **292,** 1728–1731
9. Humbert, S., Bryson, E. A., Cordelières, F. P., Connors, N. C., Datta, S. R., Finkbeiner, S., Greenberg, M. E., and Saudou, F. (2002) The IGF-1/Akt pathway is neuroprotective in Huntington's disease and involves Huntingtin phosphorylation by Akt. *Dev. Cell* **2,** 831–837
10. Huang, J. F., Chuang, Y. H., Dai, C. Y., Yu, M. L., Huang, C. F., Hsiao, P. J., Hsieh, M. Y., Huang, C. I., Yeh, M. L., Yang, J. F., Lin, Z. Y., Chen, S. C., and Chuang, W. L. (2011) Hepatic Akt expression correlates with advanced fibrosis in patients with chronic hepatitis C infection. *Hepatol. Res.* **41,** 430–436
11. Lu, Y., Azad, N., Wang, L., Iyer, A. K., Castranova, V., Jiang, B. H., and Rojanasakul, Y. (2010) Phosphatidylinositol-3-kinase/akt regulates bleomycin-induced fibroblast proliferation and collagen production. *Am. J. Respir. Cell Mol. Biol.* **42,** 432–441
12. Li, L. F., Liao, S. K., Huang, C. C., Hung, M. J., and Quinn, D. A. (2008) Serine/threonine kinase-protein kinase B and extracellular signal-regulated kinase regulate ventilator-induced pulmonary fibrosis after bleomycin-induced acute lung injury: a prospective, controlled animal experiment. *Crit. Care* **12,** R103
13. Xia, H., Diebold, D., Nho, R., Perlman, D., Kleidon, J., Kahm, J., Avdulov, S., Peterson, M., Nerva, J., Bitterman, P., and Henke, C. (2008) Pathological integrin signaling enhances proliferation of primary lung fibroblasts from patients with idiopathic pulmonary fibrosis. *J. Exp. Med.* **205,** 1659–1672
14. Vittal, R., Horowitz, J. C., Moore, B. B., Zhang, H., Martinez, F. J., Toews, G. B., Standiford, T. J., and Thannickal, V. J. (2005) Modulation of prosurvival signaling in fibroblasts by a protein kinase inhibitor protects against fibrotic tissue injury. *Am. J. Pathol.* **166,** 367–375
15. Le Cras, T. D., Korfhagen, T. R., Davidson, C., Schmidt, S., Fenchel, M., Ikegami, M., Whitsett, J. A., and Hardie, W. D. (2010) Inhibition of PI3K by PX-866 prevents transforming growth factor-α-induced pulmonary fibrosis. *Am. J. Pathol.* **176,** 679–686

16. Carano, A., Teitelbaum, S. L., Konsek, J. D., Schlesinger, P. H., and Blair, H. C. (1990) Bisphosphonates directly inhibit the bone resorption activity of isolated avian osteoclasts *in vitro*. *J. Clin. Invest.* **85,** 456–461
17. Gardner, M. J., Hall, N., Fung, E., White, O., Berriman, M., Hyman, R. W., Carlton, J. M., Pain, A., Nelson, K. E., Bowman, S., Paulsen, I. T., James, K., Eisen, J. A., Rutherford, K., Salzberg, S. L., Craig, A., Kyes, S., Chan, M. S., Nene, V., Shallom, S. J., Suh, B., Peterson, J., Angiuoli, S., Pertea, M., Allen, J., Selengut, J., Haft, D., Mather, M. W., Vaidya, A. B., Martin, D. M., Fairlamb, A. H., Fraunholz, M. J., Roos, D. S., Ralph, S. A., McFadden, G. I., Cummings, L. M., Subramanian, G. M., Mungall, C., Venter, J. C., Carucci, D. J., Hoffman, S. L., Newbold, C., Davis, R. W., Fraser, C. M., and Barrell, B. (2002) Genome sequence of the human malaria parasite *Plasmodium falciparum*. *Nature* **419,** 498–511
18. del Real, G., Jiménez-Baranda, S., Mira, E., Lacalle, R. A., Lucas, P., Gómez-Moutón, C., Alegret, M., Peña, J. M., Rodríguez-Zapata, M., Alvarez-Mon, M., Martínez, A. C., and Mañes, S. (2004) Statins inhibit HIV-1 infection by down-regulating Rho activity. *J. Exp. Med.* **200,** 541–547
19. Jiang, K., Coppola, D., Crespo, N. C., Nicosia, S. V., Hamilton, A. D., Sebti, S. M., and Cheng, J. Q. (2000) The phosphoinositide 3-OH kinase/AKT2 pathway as a critical target for farnesyltransferase inhibitor-induced apoptosis. *Mol. Cell. Biol.* **20,** 139–148
20. Kazi, A., Carie, A., Blaskovich, M. A., Bucher, C., Thai, V., Moulder, S., Peng, H., Carrico, D., Pusateri, E., Pledger, W. J., Berndt, N., Hamilton, A., and Sebti, S. M. (2009) Blockade of protein geranylgeranylation inhibits Cdk2-dependent p27Kip1 phosphorylation on Thr187 and accumulates p27Kip1 in the nucleus: implications for breast cancer therapy. *Mol. Cell. Biol.* **29,** 2254–2263
21. Sun, J., Ohkanda, J., Coppola, D., Yin, H., Kothare, M., Busciglio, B., Hamilton, A. D., and Sebti, S. M. (2003) Geranylgeranyltransferase I inhibitor GGTI-2154 induces breast carcinoma apoptosis and tumor regression in H-Ras transgenic mice. *Cancer Res.* **63,** 8922–8929
22. Ridley, A. J., Paterson, H. F., Johnston, C. L., Diekmann, D., and Hall, A. (1992) The small GTP-binding protein rac regulates growth factor-induced membrane ruffling. *Cell* **70,** 401–410
23. Reiss, Y., Goldstein, J. L., Seabra, M. C., Casey, P. J., and Brown, M. S. (1990) Inhibition of purified p21ras farnesyl:protein transferase by Cys-AAX tetrapeptides. *Cell* **62,** 81–88
24. Osborn-Heaford, H. L., Ryan, A. J., Murthy, S., Racila, A. M., He, C., Sieren, J. C., Spitz, D. R., and Carter, A. B. (2012) Mitochondrial Rac1 GTPase import and electron transfer from cytochrome *c* are required for pulmonary fibrosis. *J. Biol. Chem.* **287,** 3301–3312
25. Chen, Z., Sun, J., Pradines, A., Favre, G., Adnane, J., and Sebti, S. M. (2000) Both farnesylated and geranylgeranylated RhoB inhibit malignant transformation and suppress human tumor growth in nude mice. *J. Biol. Chem.* **275,** 17974–17978
26. Du, W., and Prendergast, G. C. (1999) Geranylgeranylated RhoB mediates suppression of human tumor cell growth by farnesyltransferase inhibitors. *Cancer Res.* **59,** 5492–5496
27. Miquel, K., Pradines, A., Sun, J., Qian, Y., Hamilton, A. D., Sebti, S. M., and Favre, G. (1997) GGTI-298 induces G0-G1 block and apoptosis, whereas FTI-277 causes G2-M enrichment in A549 cells. *Cancer Res.* **57,** 1846–1850
28. Hawkins, P. T., Eguinoa, A., Qiu, R. G., Stokoe, D., Cooke, F. T., Walters, R., Wennström, S., Claesson-Welsh, L., Evans, T., and Symons, M. (1995) PDGF stimulates an increase in GTP-Rac via activation of phosphoinositide 3-kinase. *Curr. Biol.* **5,** 393–403
29. Xue, Y., Li, N. L., Yang, J. Y., Chen, Y., Yang, L. L., and Liu, W. C. (2011) Phosphatidylinositol 3′-kinase signaling pathway is essential for Rac1-induced hypoxia-inducible factor-1α and vascular endothelial growth factor expression. *Am. J. Physiol. Heart Circ. Physiol.* **300,** H2169–H2176
30. Ozaki, M., Haga, S., Zhang, H. Q., Irani, K., and Suzuki, S. (2003) Inhibition of hypoxia/reoxygenation-induced oxidative stress in HGF-stimulated antiapoptotic signaling: role of PI3-K and Akt kinase upon rac1. *Cell Death Differ.* **10,** 508–515
31. Kwon, T., Kwon, D. Y., Chun, J., Kim, J. H., and Kang, S. S. (2000) Akt protein kinase inhibits Rac1-GTP binding through phosphorylation at serine 71 of Rac1. *J. Biol. Chem.* **275,** 423–428
32. Kuijk, L. M., Beekman, J. M., Koster, J., Waterham, H. R., Frenkel, J., and Coffer, P. J. (2008) HMG-CoA reductase inhibition induces IL-1β release through Rac1/PI3K/PKB-dependent caspase-1 activation. *Blood* **112,** 3563–3573
33. Lin, C. H., Cheng, H. W., Ma, H. P., Wu, C. H., Hong, C. Y., and Chen, B. C. (2011) Thrombin induces NF-κB activation and IL-8/CXCL8 expression in lung epithelial cells by a Rac1-dependent PI3K/Akt pathway. *J. Biol. Chem.* **286,** 10483–10494
34. Murthy, S., Ryan, A., He, C., Mallampalli, R. K., and Carter, A. B. (2010) Rac1-mediated mitochondrial H2O2 generation regulates MMP-9 gene expression in macrophages via inhibition of SP-1 and AP-1. *J. Biol. Chem.* **285,** 25062–25073
35. He, C., Murthy, S., McCormick, M. L., Spitz, D. R., Ryan, A. J., and Carter, A. B. (2011) Mitochondrial Cu,Zn-superoxide dismutase mediates pulmonary fibrosis by augmenting H_2O_2 generation. *J. Biol. Chem.* **286,** 15597–15607
36. Tephly, L. A., and Carter, A. B. (2007) Constitutive NADPH oxidase and increased mitochondrial respiratory chain activity regulate chemokine gene expression. *Am. J. Physiol. Lung Cell Mol. Physiol.* **293,** L1143–L1155
37. Shull, L. W., Wiemer, A. J., Hohl, R. J., and Wiemer, D. F. (2006) Synthesis and biological activity of isoprenoid bisphosphonates. *Bioorg. Med. Chem.* **14,** 4130–4136
38. Wasko, B. M., Dudakovic, A., and Hohl, R. J. (2011) Bisphosphonates induce autophagy by depleting geranylgeranyl diphosphate. *J. Pharmacol. Exp. Ther.* **337,** 540–546
39. Murthy, S., Adamcakova-Dodd, A., Perry, S. S., Tephly, L. A., Keller, R. M., Metwali, N., Meyerholz, D. K., Wang, Y., Glogauer, M., Thorne, P. S., and Carter, A. B. (2009) Modulation of reactive oxygen species by Rac1 or catalase prevents asbestos-induced pulmonary fibrosis. *Am. J. Physiol. Lung Cell Mol. Physiol.* **297,** L846–L855
40. He, C., Ryan, A. J., Murthy, S., and Carter, A. B. (2013) Accelerated development of pulmonary fibrosis via Cu,Zn-superoxide dismutase-induced alternative activation of macrophages. *J. Biol. Chem.* **288,** 20745–20757
41. Carmona, G., Göttig, S., Orlandi, A., Scheele, J., Bäuerle, T., Jugold, M., Kiessling, F., Henschler, R., Zeiher, A. M., Dimmeler, S., and Chavakis, E. (2009) Role of the small GTPase Rap1 for integrin activity regulation in endothelial cells and angiogenesis. *Blood* **113,** 488–497
42. Zins, K., Lucas, T., Reichl, P., Abraham, D., and Aharinejad, S. (2013) A Rac1/Cdc42 GTPase-specific small molecule inhibitor suppresses growth of primary human prostate cancer xenografts and prolongs survival in mice. *PLoS One* **8,** e74924
43. Guo, F., Cancelas, J. A., Hildeman, D., Williams, D. A., and Zheng, Y. (2008) Rac GTPase isoforms Rac1 and Rac2 play a redundant and crucial role in T-cell development. *Blood* **112,** 1767–1775
44. Zeng, P. Y., Rane, N., Du, W., Chintapalli, J., and Prendergast, G. C. (2003) Role for RhoB and PRK in the suppression of epithelial cell transformation by farnesyltransferase inhibitors. *Oncogene* **22,** 1124–1134
45. Goldstein, J. L., and Brown, M. S. (1990) Regulation of the mevalonate pathway. *Nature* **343,** 425–430
46. Dan, H. C., Jiang, K., Coppola, D., Hamilton, A., Nicosia, S. V., Sebti, S. M., and Cheng, J. Q. (2004) Phosphatidylinositol-3-OH kinase/AKT and survivin pathways as critical targets for geranylgeranyltransferase I inhibitor-induced apoptosis. *Oncogene* **23,** 706–715
47. Arranz, A., Doxaki, C., Vergadi, E., Martinez de la Torre, Y., Vaporidi, K., Lagoudaki, E. D., Ieronymaki, E., Androulidaki, A., Venihaki, M., Margioris, A. N., Stathopoulos, E. N., Tsichlis, P. N., and Tsatsanis, C. (2012) Akt1 and Akt2 protein kinases differentially contribute to macrophage polarization. *Proc. Natl. Acad. Sci. U.S.A.* **109,** 9517–9522
48. Rauh, M. J., Ho, V., Pereira, C., Sham, A., Sly, L. M., Lam, V., Huxham, L., Minchinton, A. I., Mui, A., and Krystal, G. (2005) SHIP represses the generation of alternatively activated macrophages. *Immunity* **23,** 361–374
49. Martin, M., Schifferle, R. E., Cuesta, N., Vogel, S. N., Katz, J., and Michalek, S. M. (2003) Role of the phosphatidylinositol 3 kinase-Akt pathway in the regulation of IL-10 and IL-12 by *Porphyromonas gingivalis* lipopolysaccharide. *J. Immunol.* **171,** 717–725
50. Jain, M., Rivera, S., Monclus, E. A., Synenki, L., Zirk, A., Eisenbart, J., Feghali-Bostwick, C., Mutlu, G. M., Budinger, G. R., and Chandel, N. S. (2013) Mitochondrial reactive oxygen species regulate transforming growth factor-β signaling. *J. Biol. Chem.* **288,** 770–777

51. Chensue, S. W., Warmington, K., Ruth, J. H., Lukacs, N., and Kunkel, S. L. (1997) Mycobacterial and schistosomal antigen-elicited granuloma formation in IFN-gamma and IL-4 knockout mice: analysis of local and regional cytokine and chemokine networks. *J. Immunol.* **159,** 3565–3573
52. Daley, J. M., Brancato, S. K., Thomay, A. A., Reichner, J. S., and Albina, J. E. (2010) The phenotype of murine wound macrophages. *J Leukoc. Biol.* **87,** 59–67
53. Duffield, J. S., Forbes, S. J., Constandinou, C. M., Clay, S., Partolina, M., Vuthoori, S., Wu, S., Lang, R., and Iredale, J. P. (2005) Selective depletion of macrophages reveals distinct, opposing roles during liver injury and repair. *J. Clin. Invest.* **115,** 56–65
54. Pechkovsky, D. V., Prasse, A., Kollert, F., Engel, K. M., Dentler, J., Luttmann, W., Friedrich, K., Müller-Quernheim, J., and Zissel, G. (2010) Alternatively activated alveolar macrophages in pulmonary fibrosis-mediator production and intracellular signal transduction. *Clin. Immunol.* **137,** 89–101
55. Shechter, R., Miller, O., Yovel, G., Rosenzweig, N., London, A., Ruckh, J., Kim, K. W., Klein, E., Kalchenko, V., Bendel, P., Lira, S. A., Jung, S., and Schwartz, M. (2013) Recruitment of beneficial M2 macrophages to injured spinal cord is orchestrated by remote brain choroid plexus. *Immunity* **38,** 555–569
56. Nogueira, V., Park, Y., Chen, C. C., Xu, P. Z., Chen, M. L., Tonic, I., Unterman, T., and Hay, N. (2008) Akt determines replicative senescence and oxidative or oncogenic premature senescence and sensitizes cells to oxidative apoptosis. *Cancer Cell* **14,** 458–470
57. Dolado, I., and Nebreda, A. R. (2008) AKT and oxidative stress team up to kill cancer cells. *Cancer Cell* **14,** 427–429
58. Hollander, M. C., Maier, C. R., Hobbs, E. A., Ashmore, A. R., Linnoila, R. I., and Dennis, P. A. (2011) Akt1 deletion prevents lung tumorigenesis by mutant K-ras. *Oncogene* **30,** 1812–1821
59. Vasudevan, K. M., and Garraway, L. A. (2010) AKT signaling in physiology and disease. *Curr. Top. Microbiol. Immunol.* **347,** 105–133
60. Chang, H. W., Aoki, M., Fruman, D., Auger, K. R., Bellacosa, A., Tsichlis, P. N., Cantley, L. C., Roberts, T. M., and Vogt, P. K. (1997) Transformation of chicken cells by the gene encoding the catalytic subunit of PI 3-kinase. *Science* **276,** 1848–1850
61. Chen, H. K., Fernandez-Funez, P., Acevedo, S. F., Lam, Y. C., Kaytor, M. D., Fernandez, M. H., Aitken, A., Skoulakis, E. M., Orr, H. T., Botas, J., and Zoghbi, H. Y. (2003) Interaction of Akt-phosphorylated ataxin-1 with 14-3-3 mediates neurodegeneration in spinocerebellar ataxia type 1. *Cell* **113,** 457–468
62. Georgescu, M. M., Kirsch, K. H., Akagi, T., Shishido, T., and Hanafusa, H. (1999) The tumor-suppressor activity of PTEN is regulated by its carboxyl-terminal region. *Proc. Natl. Acad. Sci. U.S.A.* **96,** 10182–10187
63. Samuels, Y., Diaz, L. A., Jr., Schmidt-Kittler, O., Cummins, J. M., Delong, L., Cheong, I., Rago, C., Huso, D. L., Lengauer, C., Kinzler, K. W., Vogelstein, B., and Velculescu, V. E. (2005) Mutant PIK3CA promotes cell growth and invasion of human cancer cells. *Cancer Cell* **7,** 561–573
64. Danesh, F. R., Sadeghi, M. M., Amro, N., Philips, C., Zeng, L., Lin, S., Sahai, A., and Kanwar, Y. S. (2002) 3-Hydroxy-3-methylglutaryl CoA reductase inhibitors prevent high glucose-induced proliferation of mesangial cells via modulation of Rho GTPase/p21 signaling pathway: Implications for diabetic nephropathy. *Proc. Natl. Acad. Sci. U.S.A.* **99,** 8301–8305
65. Brodersen, P., Sakvarelidze-Achard, L., Schaller, H., Khafif, M., Schott, G., Bendahmane, A., and Voinnet, O. (2012) Isoprenoid biosynthesis is required for miRNA function and affects membrane association of ARGONAUTE 1 in *Arabidopsis*. *Proc. Natl. Acad. Sci. U.S.A.* **109,** 1778–1783
66. Chung, C. Y., Potikyan, G., and Firtel, R. A. (2001) Control of cell polarity and chemotaxis by Akt/PKB and PI3 kinase through the regulation of PAKa. *Mol. Cell* **7,** 937–947
67. Tang, Y., Zhou, H., Chen, A., Pittman, R. N., and Field, J. (2000) The Akt proto-oncogene links Ras to Pak and cell survival signals. *J. Biol. Chem.* **275,** 9106–9109
68. Rodriguez-Viciana, P., Warne, P. H., Khwaja, A., Marte, B. M., Pappin, D., Das, P., Waterfield, M. D., Ridley, A., and Downward, J. (1997) Role of phosphoinositide 3-OH kinase in cell transformation and control of the actin cytoskeleton by Ras. *Cell* **89,** 457–467
69. Rosenson, R. S., and Tangney, C. C. (1998) Antiatherothrombotic properties of statins: implications for cardiovascular event reduction. *JAMA* **279,** 1643–1650
70. Wong, W. B., Lin, V. W., Boudreau, D., and Devine, E. B. (2013) Statins in the prevention of dementia and Alzheimer's disease: a meta-analysis of observational studies and an assessment of confounding. *Pharmacoepidemiol. Drug Saf.* **22,** 345–358
71. Merx, M. W., Liehn, E. A., Graf, J., van de Sandt, A., Schaltenbrand, M., Schrader, J., Hanrath, P., and Weber, C. (2005) Statin treatment after onset of sepsis in a murine model improves survival. *Circulation* **112,** 117–124
72. Krepkiy, D., and Miziorko, H. M. (2004) Identification of active site residues in mevalonate diphosphate decarboxylase: implications for a family of phosphotransferases. *Protein Sci.* **13,** 1875–1881
73. Dephoure, N., Zhou, C., Villén, J., Beausoleil, S. A., Bakalarski, C. E., Elledge, S. J., and Gygi, S. P. (2008) A quantitative atlas of mitotic phosphorylation. *Proc. Natl. Acad. Sci. U.S.A.* **105,** 10762–10767
74. Obata, T., Yaffe, M. B., Leparc, G. G., Piro, E. T., Maegawa, H., Kashiwagi, A., Kikkawa, R., and Cantley, L. C. (2000) Peptide and protein library screening defines optimal substrate motifs for AKT/PKB. *J. Biol. Chem.* **275,** 36108–36115
75. Redente, E. F., Keith, R. C., Janssen, W., Henson, P. M., Ortiz, L. A., Downey, G. P., Bratton, D. L., and Riches, D. W. (2014) Tumor necrosis factor-α accelerates the resolution of established pulmonary fibrosis in mice by targeting profibrotic lung macrophages. *Am. J. Respir. Cell Mol. Biol.* **50,** 825–837
76. Weigert, A., Johann, A. M., von Knethen, A., Schmidt, H., Geisslinger, G., and Brüne, B. (2006) Apoptotic cells promote macrophage survival by releasing the antiapoptotic mediator sphingosine-1-phosphate. *Blood* **108,** 1635–1642